applied sciences

MDPI

*Review*

# A Review of Femtosecond Laser-Induced Emission Techniques for Combustion and Flow Field Diagnostics

**Bo Li [1], Dayuan Zhang [1], Jixu Liu [1], Yifu Tian [1], Qiang Gao [1,*] and Zhongshan Li [1,2]**

[1] State Key Laboratory of Engines, Tianjin University, Tianjin 300072, China; boli@tju.edu.cn (B.L.); 2015201040@tju.edu.cn (D.Z.); jixuliu@tju.edu.cn (J.L.); tianyifu@tju.edu.cn (Y.T.); zhongshan.li@forbrf.lth.se (Z.L.)

[2] Division of Combustion Physics, Lund University, S-22100 Lund, Sweden

* Correspondence: qiang.gao@tju.edu.cn; Tel.: +86-022-2740-7623-8022

Received: 27 March 2019; Accepted: 6 May 2019; Published: 9 May 2019


**Abstract:** The applications of femtosecond lasers to the diagnostics of combustion and flow field have recently attracted increasing interest. Many novel spectroscopic methods have been developed in obtaining non-intrusive measurements of temperature, velocity, and species concentrations with unprecedented possibilities. In this paper, several applications of femtosecond-laser-based incoherent techniques in the field of combustion diagnostics were reviewed, including two-photon femtosecond laser-induced fluorescence (fs-TPLIF), femtosecond laser-induced breakdown spectroscopy (fs-LIBS), filament-induced nonlinear spectroscopy (FINS), femtosecond laser-induced plasma spectroscopy (FLIPS), femtosecond laser electronic excitation tagging velocimetry (FLEET), femtosecond laser-induced cyano chemiluminescence (FLICC), and filamentary anemometry using femtosecond laser-extended electric discharge (FALED). Furthermore, prospects of the femtosecond-laser-based combustion diagnostic techniques in the future were analyzed and discussed to provide a reference for the relevant researchers.

**Keywords:** combustion diagnostic; femtosecond laser; two-photon femtosecond laser-induced fluorescence; femtosecond laser-induced breakdown spectroscopy; femtosecond laser electronic excitation tagging; filament-induced nonlinear spectroscopy; femtosecond laser-induced plasma spectroscopy

## 1. Introduction

Development of advanced combustion technologies with high efficiency and low emission requires an understanding of the complex processes involving multi-scale kinetic reactions and turbulent flows. Numerous key parameters and information rely on accurate diagnostics techniques. Conventional diagnostic techniques include pressure measurement with sensors [1], velocity measurement with pitot tubes [2], and temperature measurement with thermocouples [3]. These methods, however, are all intrusive and have profound interference to combustion and flow fields, and the information extracted might be invalid, especially when high turbulence gets involved, so instantaneous measurements are needed. The advent of laser-based techniques dramatically promotes the development of diagnostic tools in these fields [4,5], which provides more reliable and new information to support further research. Compared with intrusive techniques, laser-based techniques can prominently reduce or even avoid the interference. In addition, high sensitivity, high temporal, and spatial resolution can be obtained in real time, and simultaneous multi-parameter measurements can also be achieved. Aldén [4] mentioned that "laser diagnostic techniques have for more than 30 years added very valuable input for a deepened understanding of combustion processes". Kohse-Höinghaus [5] further stated

that laser-based diagnostic technique "is the only way to 'spy' on the fundamentals of combustion inside". The light source is the core component of laser diagnostic techniques, a typical example of which is nanosecond (ns) lasers. Over recent decades, ns-laser diagnostics have been widely adopted in characterizing many aspects of combustion and flow fields, e.g., flow and flame structure visualization [6], species measurement [7], temperature measurement [8], velocity measurement [9], and soot characteristics analysis [10]. Various ns-laser diagnostics, however, all have their own limitations. For example, in two-photon laser-induced fluorescence (TPLIF), it is hard to find the balance between high laser fluence, which is needed to compensate for the reduced absorption cross-section, and the laser-induced photolysis, which is proportional to laser fluence and is something we would like to avoid. Other challenges faced by ns-laser techniques include measuring in the near-wall region and in the sooty environment, and so on. Hence, it is necessary to develop new techniques to solve the problems mentioned above.

The advent of femtosecond (fs) lasers [11] has significantly enriched the laser-based diagnostic techniques. At present, there are many commercial fs lasers, and the average power of the fs laser pulse could reach the order of tens of watts, and the repetition rate can reach the order of GHz. Among them, the most commonly used fs laser for diagnostics in combustion and flow field is the Ti:sapphire laser system, whose wavelength centered at ~800 nm with a pulse duration of ~45 fs, a pulse energy of 8 mJ, and a repetition rate of 1 kHz. Compared with ns lasers, fs lasers have the characteristics of a narrower pulse duration, a higher peak power, and a broader line width. Hence, when fs lasers interact with gases, different behaviors and phenomena will be observed, such as fs laser filamentation [12,13]. To understand these behaviors and phenomena, a direct and convenient way is to monitor the emission that arises from the volume of the fs laser-gas interaction. By doing so, we can extract information from the gas field of interest, which will not be stimulated by ns lasers. Hopefully, this will shed light on solving the difficulties faced by ns-laser diagnostic techniques. For instance, femtosecond multiphoton laser-induced fluorescence (fs-MPLIF) has the advantages of high multiphoton excitation efficiency and, at the same time, low photolysis interference. Hence, the primary purpose of this paper is to discuss in detail these advantages along with the emerging diagnostic techniques based on them and to introduce the applications of fs laser-induced emission techniques for combustion and flow field diagnostics.

In this paper, we put these incoherent techniques based on fs laser-induced emission into four categories. In Section 2, we focus on a resonant excitation technique: Femtosecond two-photon laser-induced fluorescence (fs-TPLIF). In Section 3, we introduce a non-resonant excitation technique: Femtosecond laser-induced breakdown spectroscopy (fs-LIBS). In Section 4, we describe techniques that rely on fs laser-induced filamentation: Filament-induced nonlinear spectroscopy (FINS), femtosecond laser-induced plasma spectroscopy (FLIPS), femtosecond laser electronic excitation tagging (FLEET) and femtosecond laser-induced cyano chemiluminescence (FLICC). In Section 5, we outline a technique based on fs laser-guiding electric discharge: Filamentary anemometry using femtosecond laser-extended electric discharge (FALED). The paper is closed with a summary in Section 6.

## 2. Femtosecond Two-Photon Laser-Induced Fluorescence (fs-TPLIF)

Laser-induced fluorescence (LIF) is one of the most common techniques for combustion diagnostics [7], which uses a resonant laser beam to excite a selected transition from a special molecule (or atom) to a higher excited state and detects the induced fluorescence. Various combustion intermediate species can be measured by LIF [14,15]. Based on fluorescence imaging, two-dimensional visualization can also be achieved by planner LIF [16].

For LIF measurements, one-photon excitation is preferred, since it has a linear response and high absorption cross-section. However, many key combustion intermediates, such as atomic hydrogen (H) [17], atomic oxygen (O) [18] and carbon dioxide (CO) [19], have a large energy gap between the ground and the first excited electronic states, which makes one-photon LIF impossible as the wavelength falls into the region of vacuum-ultraviolet (VUV). To address this complication, researchers

developed a two-photon excitation scheme. Two-photon laser-induced fluorescence (TPLIF) was first demonstrated for H and deuterium measurements by Bokor et al. [20], and then it was applied to detect many other species, including O [21–23] and N [22]. A limitation of two-photon excitation is that high laser fluence is required in order to overcome the issue of small absorption cross-section. The high laser fluence could cause significant photo-dissociation. For example, in TPLIF detection of H, a substantial amount of additional H can be produced via photodissociation [24] of some hydrogen-containing radicals, such as $H_2O_2$ [25] and $CH_3$ [26], which makes it difficult to distinguish the natively generated H in the flame and the photolytic H. Even if the photolytic products are different from the species of interest, they may also cause interference. For example, when performing CO-TPLIF measurements in a sooty flame, the ns-laser at 230 nm, which is used to excite CO molecules, will generate photolytic $C_2$ radicals. Moreover, the so-called Swan-band emissions from $C_2$ will interfere with the CO detection, since they partially overlap with the CO fluorescence.

To circumvent the above-mentioned issues, researchers use fs lasers in place of ns lasers. By assuming that the molecular transitions have a linewidth much narrower than the excitation laser energy distribution [27], the efficiency of two-photon excitation can be expressed as

$$S_{\mathrm{LIF}} \propto \sigma_0 \cdot I_0^2 \frac{1}{c_\omega \cdot c_t}, \tag{1}$$

where $S_{\mathrm{LIF}}$ is the fluorescence signal, $\sigma_0$ is the two-photon rate coefficient, $I_0$ is the laser pulse energy of the excitation laser, $c_\omega$ is the laser spectral linewidth of the laser, and $c_t$ is the laser pulse duration, so the relative TPLIF efficiency can be estimated by the product of $c_t \cdot c_\omega$ of the excitation laser pulse. For a Fourier transform limited (FTL) laser pulse, $c_t \cdot c_\omega$ is a constant and has the smallest value, which is the most favorable for the two-photon excitation. Most fs laser pulses are close to FTL, while for most ns or picosecond (ps) laser pulses, the $c_t \cdot c_\omega$ values are generally larger by a factor of around 100. For detection of molecular species, the possibility of a simultaneous excitation of the whole vibration band (or even including some hot bands) forms another extra advantage of fs-TPLIF in contrast to the ns and ps cases, where only a couple of rotational lines can be excited. This effect will be more evident in flames, where much more rotational lines and even hot vibrational bands can be populated.

Therefore, even if the pulse energy of an fs laser is two orders of magnitude lower than that of a typical ns laser, the fluorescence intensity is similar to that in ns or ps TPLIF measurements [28,29]. Considering that the photolytic interferences are often linearly proportional to the laser pulse energy, the photodissociation problem will be mitigated to a large extent for fs-TPLIF. Besides the advantage of photolytic interference suppression, the effective utilization of the whole broadband profile of the fs laser pulse due to the existence of multi photon-pairs in matching the two-photon resonant excitation has also been mentioned by Kulatilaka et al. [30].

So far, fs-TPLIF has been applied to measure various combustion intermediates and products, including molecules (e.g., CO), atoms (e.g., H and O), and radicals (e.g., OH). Inert gases (e.g., Kr and Xe) are also of interest because crucial parameters, like mixing fraction, could be extracted by measuring them. The excitation and detection strategies of the abovementioned species are listed in Table 1.

**Table 1.** Excitation and detection strategies of various species by multi-photo femtosecond laser induced fluorescence.

| Species | Excitation | | Detection | | Ref. |
|---|---|---|---|---|---|
| | Wavelength | Transition | Wavelength | Transition | |
| OH | 620 nm*2 | $A^2\Sigma^+ \leftarrow X^2\Pi$ | ~310 nm | $A^2\Sigma^+ \rightarrow X^2\Pi$ | [31,32] |
| CO | 230 nm*2 | $B^1\Sigma^+ \leftarrow X^1\Sigma^+$ | 400–600 nm | $B^1\Sigma^+ \rightarrow A^1\Pi^+$ | [27,33–38] |
| | 230 nm*2 | $B^1\Sigma^+ \leftarrow X^1\Sigma^+$ | 280–380 nm | $b^3\Sigma^+ \rightarrow a^3\Pi$ | [34] |
| H | 205 nm*2 | $n = 3 \leftarrow n = 1$ | 656 nm | $n = 3 \rightarrow n = 2$ | [30,39–50] |
| | 307 nm*3 | $n = 3 \leftarrow n = 1$ | 656 nm | $n = 3 \rightarrow n = 2$ | [40,47] |
| | 243 nm*2 + 486 nm | $n = 4 \leftarrow n = 1$ | 656 nm | $n = 3 \rightarrow n = 2$ | [51] |
| O | 226 nm*2 | $3p^3P \leftarrow 2p^3P$ | 845 nm | $3p^3P \rightarrow 3s^3S$ | [49,52,53] |
| Kr | 204.1 nm*2 | $5p'[3/2]_2 \leftarrow 4p^6[^1s_0]$ | 826 nm | $5p'[3/2]_2 \rightarrow 5s'[1/2]_1$ | [49,50,54] |
| | 204.1 nm*2 | $5p'[3/2]_2 \leftarrow 4p^6[^1s_0]$ | 750–840 nm | | [55,56] |
| | 212.6 nm*2 | $4s^24p^55p/4s^24p^55p' \leftarrow 4s^24p^6$ | 759 nm | | [57] |
| Xe | 225 nm*2 | $6p'[3/2]_2 \leftarrow 5p^61S_0$ | 835 nm | $6p'[3/2]_2 \leftarrow 6s'[1/2]_1$ | [49,53] |

Note: Refs. [50–52,55] are measured in plasma.

The measurement of CO by fs-TPLIF was first performed by Richardson et al. [37] in a steady flame. In their research, excitation wavelength at 230.1 nm was used to induce two-photon transition ($B^1\Sigma^+ \leftarrow X^1\Sigma^+$) of CO, and fluorescence in the range of 362–516 nm was captured. Later on, this excitation scheme has been extended into high-pressure flames [34], sooty flames [34], and piloted liquid-spray flames [33]. Our group also employed this scheme in a premixed laminar jet flame [27]. A hot band (1,n) together with the conventional band (0,n) of $B^1\Sigma^+ \rightarrow A^1\Pi^+$ transitions were observed in the burned zone of the flame. As shown in Figure 1b, the $B^1\Sigma^+ \leftarrow X^1\Sigma^+(1,1)$ band was excited due to the broadband nature of the fs laser pulse. We have seen that the two vibrational bands are sensitive to temperature and can potentially be used for accurate flame temperature measurements. In addition, the CO fs-TPLIF signal recorded across the focal point of the excitation beam shows a relatively flat intensity distribution despite the steep laser intensity variation, which is beneficial for CO imaging in contrast to ns and ps TPLIF.

For atomic intermediates in combustion, fs-TPLIF has been applied to H and O measurements. Atomic hydrogen is a critical species in the combustion of hydrogen or hydrocarbon fuels [58], which gets involved in flame ignition, propagation, and extinction. The H fs-TPLIF technique was first demonstrated in combustion by Kulatilaka et al. [30,46]. In their scheme, H was excited by a 205 nm fs laser, and the subsequent $H_\alpha$ fluorescence at 656 nm from the transition $n = 3 \rightarrow n = 2$ was detected, as shown by the red line in Figure 2. This excitation scheme has also been adopted for quantitative measurements [44] and 2D imaging [45]. Another extinction scheme, shown as the blue line in Figure 2, was proposed by our group [51]. In the scheme, H is electronically excited through a two-photon process by a 243 nm laser from the ground state to its first excited state ($n = 3 \leftarrow n = 1$), where the excited H is instantaneously re-excited through another one-photon process by a relay laser (486 nm) to excited state of $n = 3$. In order to avoid the stray light interference from the 486 nm laser, the secondary fluorescence at 656 nm ($n = 3 \rightarrow n = 2$) was collected. Consequently, interference-free H imaging was achieved in a laminar jet flame. Furthermore, a three-photon (307.7 nm) excitation scheme ($n = 3 \leftarrow n = 1$) with detection fluorescence at 656 nm was demonstrated by Jain et al. [40], as shown by the green line in Figure 2.

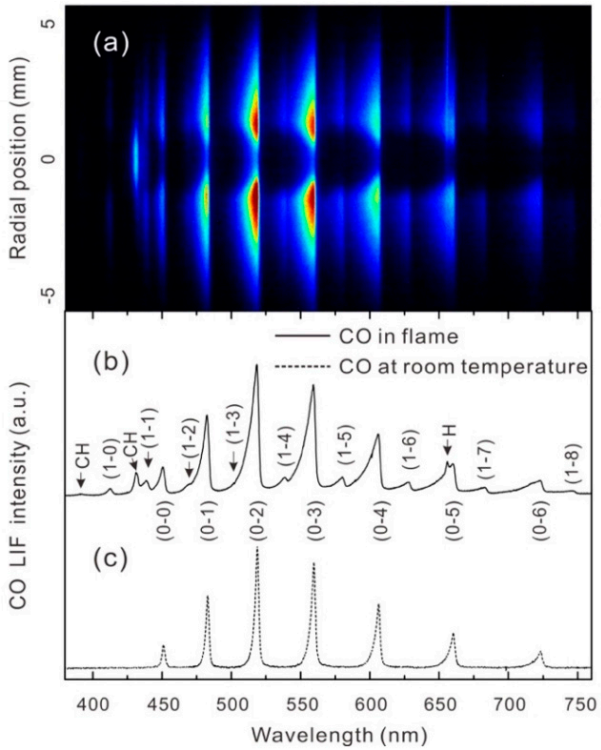


**Figure 1.** Spectra of CO femtosecond two-photon laser-induced fluorescence (fs-TPLIF): (**a**) Spatially resolved imaging spectrum recorded in a laminar premixed $CH_4$/air jet flame ($\Phi$ = 1.5); (**b**) integrated spectral curve of the flame; (**c**) spectral curve of a gas mixture of CO/$N_2$ at room temperature [27]. (© *2017 Optical Society of America*).

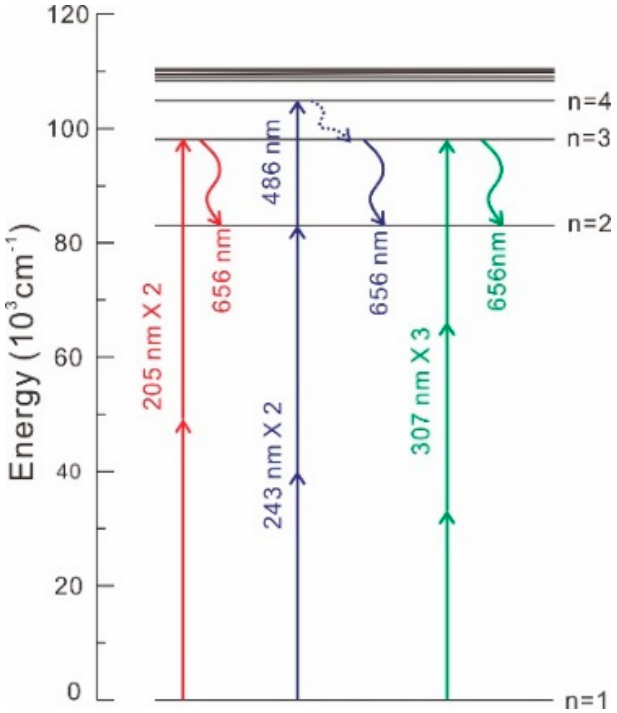


**Figure 2.** Excitation and detection strategy of atomic hydrogen using the multiphoton femtosecond laser-induced fluorescence (MP-fs-LIF).

Kulatilaka et al. [52] also performed an fs-TPLIF diagnosis for O in premixed laminar flame. An fs laser at 226 nm was used for two-photon excitation of O to its excited state ($3p^3P \leftarrow 2p^3P$), and the subsequent O fluorescence at 845 nm from the transition $3p^3P \rightarrow 3s^3S$ was detected. The advantage of fs lasers excitation over traditional ns lasers excitation in O measurements is that the photolysis of vibrationally excited $CO_2$, known as the main interference that produces additional O atoms [59], can be eliminated.

Combustion radicals can also be measured by fs-TPLIF. Hydroxyl (OH) is one of the essential combustion radicals, and OH-PLIF is widely used to visualize the reaction zone and product zone of a flame [60–63]. Different from CO, H, and O, OH can be excited with single-photon strategy. A typical single-photon OH-LIF uses an ns laser at ~283 nm to excite OH through a transition line in $A^2\Sigma^+ \leftarrow X^2\Pi$ (0, 1) band, which allows observation of the fluorescence emission from the (1, 1) and (0, 0) bands at ~310 nm [64]. There are many researches of OH-LIF, including ns-laser excitation [62,63] and ps-laser excitation [65]. Stauffer et al. [31,32] performed the fs-TPLIF of OH measurements with two-photon excitation at 620 nm. However, they did not directly observe any obvious advantages of two-photon fs-laser excitation relative to single-photon ns- or ps-laser excitation.

Femtosecond-TPLIF has also been used to measure inert gases such as Kr [54–57] and Xe [49]. Although these studies do not directly measure the combustion species, they are still relevant to combustion research. For example, fs-TPLIF imaging of Kr was achieved to measure the mixture fraction in gaseous flows [57], which is a crucial parameter in the combustion flow field. Femtosecond-TPLIF measurement of Xe was demonstrated in the plasma induced by discharges [49], which might be useful for studying the ignition behavior of flammable gases.

In summary, fs-TPLIF has shown great potential for combustion species measurements, owing to its advantages of high multi-photon efficiency and little photolysis interference. More studies are yet to be performed. For example, fs-TPLIF can be further used to measure other combustion intermediates such as atomic C [66,67] and N [22]. In addition, the technique has not been applied to measure any polyatomic molecule, such as $NH_3$ [68], which is also of great interest to the combustion community. Furthermore, two-color fs-TPLIF is another strategy that is worth trying. For single-color fs-TPLIF, only one tunable UV laser is needed, but the problem is that its pulse energy is quite limited, while for the two-color strategy, we could use two lasers at two wavelengths. Hence, we have the flexibility to choose at least one laser with strong pulse energy, e.g., from the fourth-harmonic output (200 nm) of an fs Ti:sapphire laser, and then select a tunable UV laser to match the strong laser. In doing so, the excitation efficiency might be improved.

## 3. Femtosecond Laser-Induced Breakdown Spectroscopy (fs-LIBS)

Laser-induced breakdown spectroscopy (LIBS) is broadly applied to combustion diagnostics, largely encouraged by its simplicity in terms of both experimental setup and data evaluation, which have been applied to many fields such as industry [69], chemistry [70], biology [71,72], nuclear [73], earth sciences [74–76], and cultural heritage [77]. Different from LIF, LIBS technique involves non-resonant excitation, and an ns laser with a fixed wavelength meets the demand. For the current development of ns-LIBS, readers can refer to [78,79]. In the field of combustion, LIBS is mainly used to measure the equivalence ratio. When a pulsed laser is focused at a premixed fuel/air mixture, a breakdown will be generated, which acts as a virtual measurement probe. When the assumptions of local thermal equilibrium (LTE) and optically thin plasma are satisfied [80,81], the intensities of the spectral emission lines of the plasma can be used to determine the equivalence ratio quantitatively. In most of the previous studies, the ratios of certain spectral lines of LIBS could be used to correlate and quantify mixture fraction including H (656 nm)/O (777 nm) [82–84], H (656 nm)/N (568 nm) [85], C (833 nm)/N (744 nm) [86], C (833 nm)/O (777 nm) [86], C (711 nm)/(N (745 nm)+O (777 nm)) [87], and $C_2$ (516.5 nm)/CN (388 nm) [88].

With the development of ultrafast lasers, LIBS with fs lasers as a light source (fs-LIBS) was introduced [89]. In recent years, fs-LIBS has been applied to combustion diagnostics, and it was also mainly used to measure equivalence ratio. Femtosecond-LIBS is similar to ns-LIBS. The fs laser

is focused by a spherical lens with short focal length (e.g., 65 mm focal length [90]) to generate a breakdown (or plasma) in the flow field. By measuring and analyzing the emission spectrum of the plasma, the parameters, such as equivalence ratio, can be obtained. Femtosecond-LIBS has the potential to solve some technical defects faced by traditional ns-LIBS. For example, in ns-LIBS measurements, the intrinsic unstable character of avalanche ionization will lead to volatile signal and hence, result in the instability of the equivalence ratio measurements. The situation will be even worse under high pressure or with the presence of a high level of soot [91]. Femtosecond-LIBS, on the other hand, can avoid the problem to some extent [92].

For the first time, Kotzagianni et al. [90,93] performed fs-LIBS technique in a premixed $CH_4$/air flame. They used the spectral intensity of CN at 388 nm to calibrate equivalence ratio, as shown in Figure 3, and in situ equivalent ratio measurements were realized. In addition, fs-LIBS was also applied by Couris et al. [94]. They used the intensity ratio of H (656 nm)/O (777 nm) and $C_2$ (516.5 nm)/CN (388 nm) to calibrate the fuel concentration in flames. Patnaik et al. [95] developed a multivariate analysis to understand and mitigate the measurement instability by varying the pulse duration of the light source from ns to fs. The results indicated that LIBS measurements with fs pulse excitation could reduce the instability in equivalence ratio measurements under high pressure.

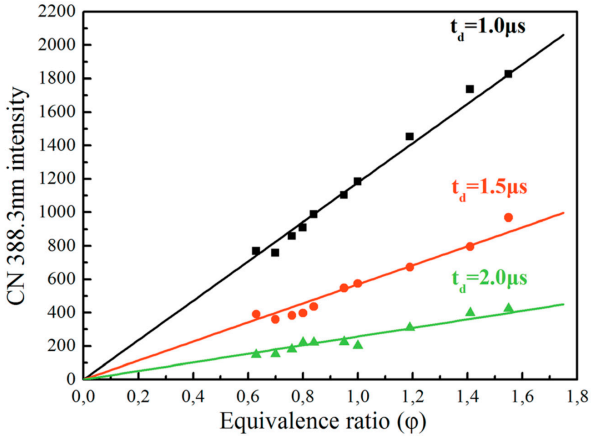


**Figure 3.** Intensity variation of the CN (388.3 nm) band as a function of the equivalence ratio at different delay times in a $CH_4$/air flame [93]. (Reproduced from Kotzagianni M., and Couris S., Femtosecond laser induced breakdown for combustion diagnostics. *Appl. Phys. Lett.* 2012, *100*, 264104, with the permission of AIP Publishing).

Although its feasibility in equivalence ratio measurements has been confirmed, more works are yet to be done to fully exploit the advantages of fs-LIBS, e.g., its capability for one-dimensional or high spatial resolution measurements. In addition, similar to ns-LIBS, drastic breakdown happens in fs-LIBS based on tight focusing of the fs laser. Therefore, the spectrum of fs-LIBS is dominated by atomic emissions, which might miss some crucial information related to molecules. Furthermore, fs-LIBS has continuum background interference [90,93], which may disturb the measurements. If using a spherical lens with long focal length, this issue will be reduced. Hence, many techniques depending on femtosecond laser-induced emission have been developed.

## 4. Femtosecond Laser-Induced Filament Emission

Different from the strong focusing in fs-LIBS, when an fs laser is focused with a longer focal length lens, the focused femtosecond laser can form a stable plasma channel in the optical medium. This phenomenon is also known as filamentation, and the plasma channel is called a filament. Femtosecond laser-induced filamentation is a unique phenomenon that appears during the propagation of a high-intensity ultrashort laser in a transparent medium. This phenomenon was first observed by Braun et al. [96] in 1995. The appearance of fs filament is due to the dynamic balance between the optical Kerr

effect-induced self-focusing and the defocusing effect of the self-generated plasma. Chin et al. [13] suggested that filament could be defined as the propagation zone where there is intensity clamping, and its length is at least several times longer than Rayleigh range.

The clamping intensity inside the plasma channel induced by fs laser is up to $10^{13}$~$10^{14}$ W/cm$^2$ [13], which is intense enough to excite atoms/molecules into higher excited states through photolysis, ionization, dissociation, and collision. Then, the excited atoms/molecules release characteristic fluorescence. Therefore, the emission spectra of the plasma channel are rich in information, and the component information of the measured flow field can be obtained qualitatively or quantitatively through spectral analysis. Such non-resonant spectroscopy techniques include filament-induced nonlinear spectroscopy (FINS) and femtosecond laser-induced plasma spectroscopy (FLIPS). In addition, the plasma channel can also excite molecules into higher excited states through laser-induced photochemical reactions, which can extend the fluorescence "lifetime". These long-life signals can be used to measure the velocity of the flow field. Such tagging velocimetry includes femtosecond laser electronic excitation tagging (FLEET) and femtosecond laser-induced cyano chemiluminescence (FLICC).

### *4.1. Spectroscopy Techniques Based on Femtosecond Laser-Induced Filament Emission*

Filament-induced nonlinear spectroscopy (FINS) is a non-resonant spectroscopy technique, which utilizes the short-lifetime signal of the fs laser-induced filament. FINS technique has already demonstrated its potential application prospect in many fields [97,98], such as remote sensing of greenhouse gases [99], pollutants measurements in atmosphere [100], humidity monitoring [101], and heavy-metal contaminants detection in water [102]. The applications of FINS in combustion diagnostics have emerged in recent years.

In 2013, Li et. al. [103] demonstrated the proof-of-concept for FINS in combustion diagnostics, and simultaneous monitoring of multiple combustion intermediates was realized in ethanol/air flame. They compared the emission spectra obtained by FINS, ns-LIBS and spontaneous emission of ethanol/air flame [104], as shown in Figure 4. They found that the signal of FINS in flame mainly results from the interaction between fs laser pulses and the combustion intermediates, such as OH, CH, and $C_2$. They expanded the application of FINS into different alkanol/air flames [105], i.e., methanol ($CH_3OH$), ethanol ($CH_3CH_2OH$), n-propanol ($CH_3(CH_2)_2OH$), n-butanol ($CH_3(CH_2)_3OH$), and n-pentanol ($CH_3(CH_2)_4OH$). Li et al. [106] also demonstrated that FINS could be utilized to sense the combustion intermediates by measuring the backward fluorescence spectra of filament emission in the flame.

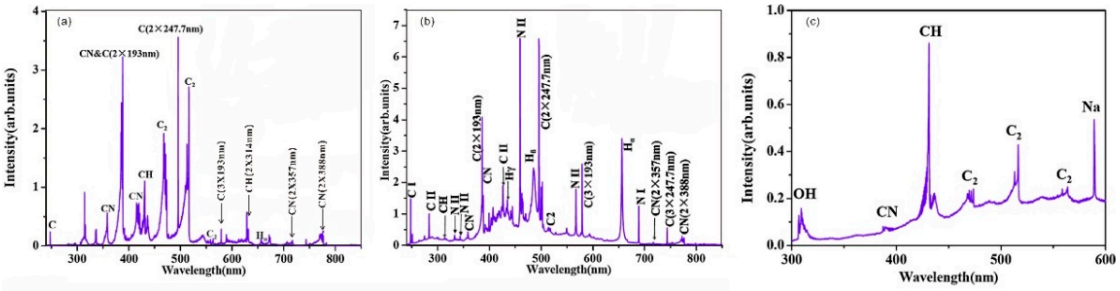


**Figure 4.** A comparison of emission spectra obtained by (**a**) femtosecond filament excitation, (**b**) nanosecond laser-induced breakdown excitation, and (**c**) without any laser excitation [104]. (Reprinted from Sensors and Actuators: B Chemical, 203, Li H., Wei X., Xu H., Chin S., Yamanouchi K., and Sun H., femtosecond laser filamentation for sensing combustion intermediates: A comparative study, 887, 2014, with permission from Elsevier; Reprinted from The Lancet, 203, Li H., Wei X., Xu H., Chin S., Yamanouchi K., and Sun H., femtosecond laser filamentation for sensing combustion intermediates: A comparative study, 887, 2014, with permission from Elsevier).

Li et al. [107] also obtained critical power and clamping intensity of filament in the combustion flow field. The results indicate that the critical power in the flame is 4–5 times smaller than the usually quoted one in air, and the clamping intensity inside the filament is roughly half of that in the air.

They also found the lasing action [108] and third-harmonic generation [109] in flame. These results and observations can provide insights into the understanding of FINS for practical applications in combustion diagnostics.

There are some advantages of FINS in the application of combustion diagnostics. First of all, FINS can measure multiple combustion intermediates simultaneously with a simple optical setup, which is based on the unique nonlinear optical phenomenon of the filament. Compared with the ns-LIBS technique, the spectra of FINS consist of not only atoms but also molecules, which provide more valuable information. Consequently, FINS can reflect the composition of the measured flow field more realistically. However, the current exploitation of FINS is not complete. For example, previous works have focused on FINS in an alcohol burner array, as shown in Figure 5, which lacks standard data such as temperature or component concentration for comparison. It is thus more meaningful to perform FINS in a standard burner, such as a McKenna burner [110].

**Figure 5.** The photo of the flame on the alcohol burner array together with the femtosecond laser-induced filament [108]. (Reproduced from Chu W., Li H., Ni J., Zeng B., Yao J., Zhang H., Li G., Jing C., Xie H., Xu H.; Yamanouchi K, and Cheng Y, Lasing action induced by femtosecond laser filamentation in ethanol flame for combustion diagnosis, with the permission of AIP Publishing).

Besides FINS, another technique called femtosecond laser-induced plasma spectroscopy (FLIPS) should also fall in this category. FLIPS can acquire component information based on quantitative spectral analysis of the plasma emission. As mentioned above, different from fs-LIBS, FLIPS generally uses an fs pulse focused lens with a longer focal length, and the clamping intensity of the generated filament is about $10^{13}$~$10^{14}$ W/cm$^2$ [12,13]. By contrast, the breakdown threshold of fs-LIBS is about $2\sim4 \times 10^{14}$ W/cm$^2$ in air at $\lambda$ = 800 nm [89,111]. As a consequence, FLIPS does not suffer from interference of continuous background and contains substantial molecular bands, which can provide more information for spectral analysis.

Hsu et al. [112] used FLIPS to achieve a stable and reliable gas sensing at elevated pressures. The results showed that the signal level of FLIPS increases with the increase of pressure while maintaining the stability in the pressure range of 1–40 bar.

Our group [113] developed FLIPS for instantaneous one-dimensional equivalence ratio measurement in a free jet with non-reacting premixed $CH_4$/air. By measuring the spatially resolved spectra of FLIPS, we found that the spectral peak area ratios of CH (431 nm)/$N_2$ (337 nm), CH (431 nm)/$N_2$ (357 nm), and CH (431 nm)/O (777 nm) can be utilized to achieve one-dimensional local equivalence ratio measurement. Among them, the CH peak at ~431 nm and the O peak at ~777 nm is strong enough to be used to achieve single-shot measurements, and a spatial resolution of 150 μm was achieved, which is important for turbulent flow fields. Figure 6 indicates the results of FLIPS technique used in both laminar and turbulent flow fields for instantaneous one-dimensional equivalence ratio measurement.

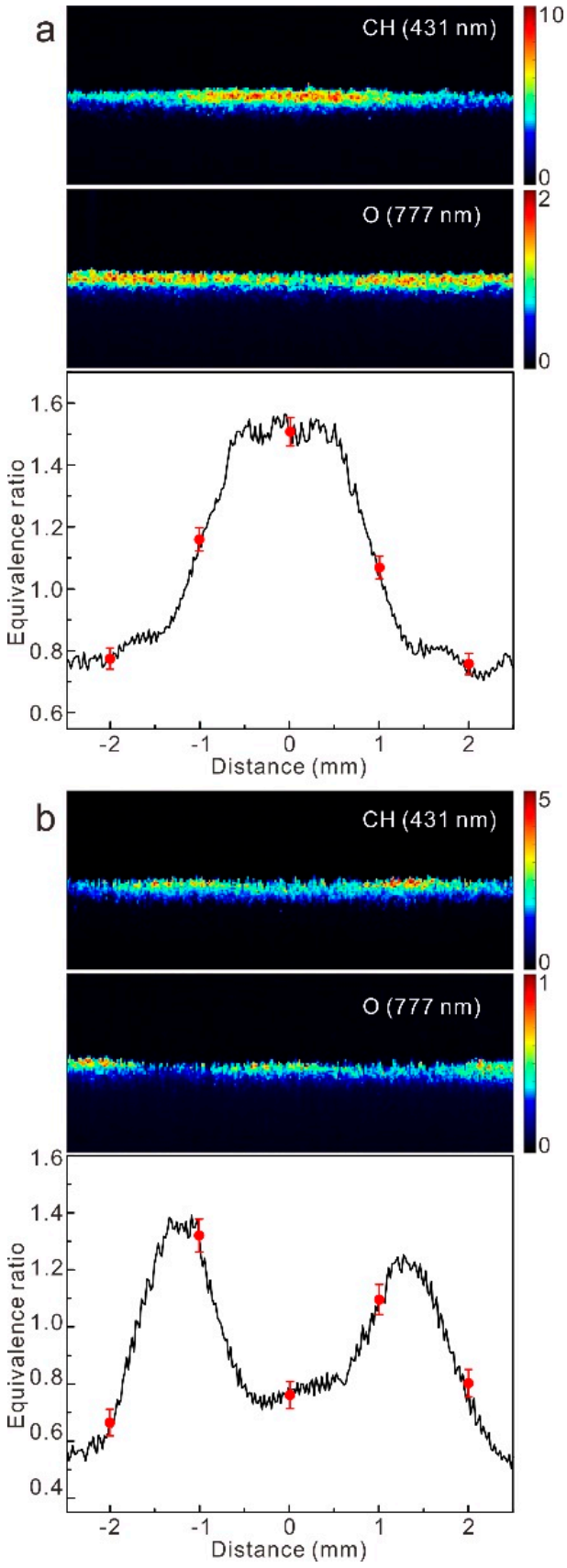


**Figure 6.** Single-shot images of femtosecond laser-induced plasma spectroscopy (FLIPS) in laminar (**a**) and turbulent (**b**) flow field with two intensified charge-coupled device (ICCD) cameras and two filters [113]. (© *2019 Optical Society of America*).

The main advantages of FLIPS are as follows. Firstly, FLIPS can achieve instantaneous one-dimensional measurement with a simple experimental setup. Secondly, the spatial resolution of FLIPS is on the order of 100 microns, which is at least one order of magnitude lower than that of ns-LIBS. Thirdly, compared with traditional ns-LIBS, FLIPS technique is free from broadband bremsstrahlung interference. Fourthly, FLIPS technique also has feasibility under high-pressure conditions.

Femtosecond laser-induced emissions can last for a while, and the filament offers a one-dimensional spatial resolution. Combining these two features, researches established another application to achieve velocity measurements in the flow field.

### *4.2. Tagging Velocimetry Based on Femtosecond Laser-Induced Emission*

Velocity measurement in the flow field is another important application of fs laser-induced filament emission. Velocity is one of the most significant parameters in the combustion flow field. Techniques that can be used for velocity measurements include invasive techniques, such as pitot tube [2] and hot wire anemometer [114], and non-invasive techniques, such as particle imaging velocimetry (PIV) [115,116], laser Doppler velocimetry (LDV) [117], and molecular tagging velocimetry (MTV) [118]. As a cutting-edge technique, MTV has developed rapidly in recent decades, and it has been extensively studied in the combustion flow field. MTV measures flow field velocity by time-of-flight analysis. The molecules in the flow field are tagged through a "write" process, which is followed by a "read" process in order to probe the tagged molecules at a known delay time. Consequently, the movement of the tagged molecules gives the velocity. MTV techniques can be categorized by whether the atomic/molecular tracer is "seeded" or "unseeded". In "seeded" MTV methods, the flow is seeded with molecules (or atoms) such as ketone [119,120], ester [121], nitric oxide [122,123], and metal atoms [124,125]. Different atomic/molecular tracers are seeded in terms of different flow fields. Therefore, these methods have a wide scope of applications and high accuracy. However, seeding of these atomic/molecular tracers is often undesirable due to expense, toxicity, corrosivity, and so on. Furthermore, when these methods are applied in the combustion flow field, it is necessary to consider whether the additional tracers have effects on the combustion reactions. Various "unseeded" MTV methods were developed as well, e.g., Raman excitation plus laser-induced electronic fluorescence (RELIEF) with $O_2$ as tracer [126,127], air photolysis and recombination tracking (APART) with NO as tracer [128], ozone tagging velocimetry (OTV) with $O_3$ as tracer [129,130], and hydroxyl tagging velocimetry (HTV) with OH as tracer [131–133]. For detailed information about MTV, readers can refer to a review [118].

Traditional MTV techniques use ns lasers as the light source. With the evolution of fs lasers and their gradual applications to the field of combustion, some velocity measurement techniques based on fs lasers have been developed, including femtosecond laser electronic excitation tagging (FLEET) and femtosecond laser-induced cyano chemiluminescence (FLICC).

FLEET is a recently developed fs-laser-based tagging velocimetry in nitrogen-containing flow field, which was proposed by Michael et al. [134]. It is the first attempt of an fs laser in gaseous flow field velocity measurement. The FLEET nitrogen tagging mechanism is shown in Figure 7. When an fs laser with a wavelength of 800 nm was focused at the nitrogen-containing flow field, the laser pulse ionized and dissociated molecular nitrogen into atomic nitrogen, which produced long-lived fluorescence as the nitrogen atoms recombined into excited electronic states of molecular nitrogen. Through imaging $N_2$ fluorescence of first positive band ($B^3\Pi_g \rightarrow A^3\Sigma_u^+$) at different delays and analyzing, the flow field velocity can be obtained. However, FLEET is a non-resonant process, as shown by the red transition of Figure 8. FLEET process requires absorption of at least eight photons to overcome the 9.8 eV [135] dissociation energy of $N_2$. As a result, in order to induce multi-photon dissociation, the femtosecond laser with an energy of several mJ is needed, which can photo-dissociate many other species, heat the probing volume, or alter local chemistry. One way to avoid these problems is to use low laser pulse energy. Therefore, selective two-photon absorptive resonance FLEET (STARFLEET) approach was developed by Jiang et al. [135–138], which significantly reduces the per-pulse energy to 30 μJ. As shown

by the blue transition in Figure 8, STARFLEET is designed to exploit the resonant excitation of the $N_2$ $a'' {}^1\Sigma_g^+ \leftarrow X1\Sigma_g^+$ transition via two-photon absorption at ~202.25 nm. Then the pre-dissociated $N_2$ at $a'' {}^1\Sigma_g^+$ absorbs the third photon, and dissociation of $N_2$ molecule happens. STARFLEET approach has the same capabilities as FLEET, but is more efficient than FLEET.

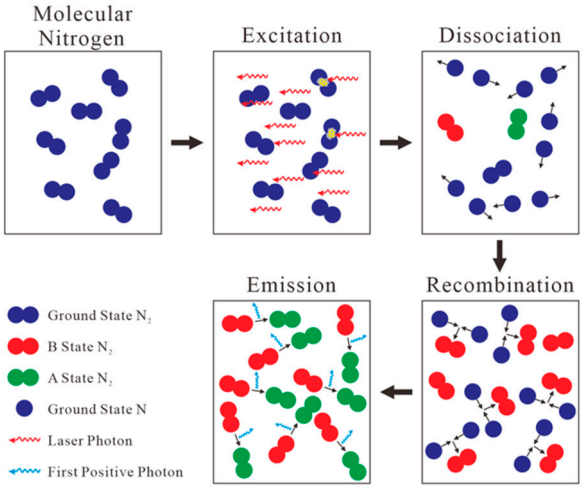


**Figure 7.** Diagram of the femtosecond laser electronic excitation tagging velocimetry (FLEET) nitrogen tagging mechanism. The incident 100 fs laser dissociates the nitrogen molecules into atoms, which subsequently recombine into the excited B state of molecular nitrogen, which emits in the red and near infrared through the first positive transition to the A state.

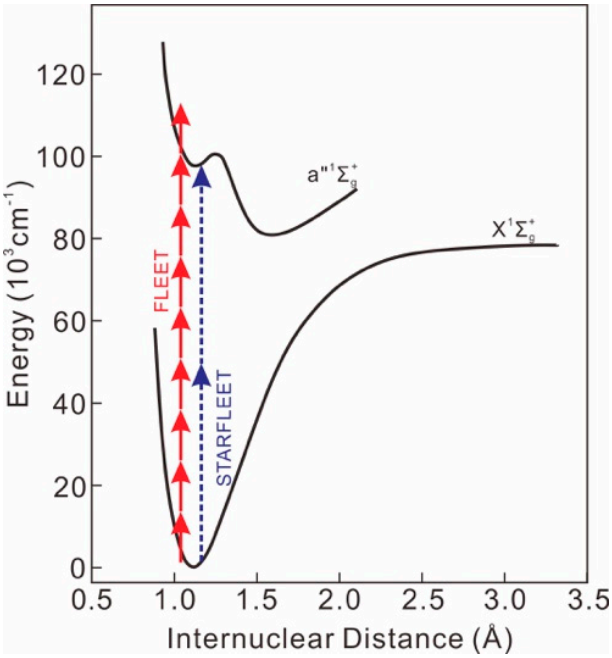


**Figure 8.** The nitrogen excitation strategy of FLEET and selective two-photon absorptive resonance FLEET (STARFLEET).

FLEET is used in a wide range of applications, including subsonic [134,139–141], transonic [136,142–144], and hypersonic [145–148] flow fields. At present, FLEET has been successfully applied in nitrogen [134,140,141,149–152], argon [139,153–155], air [141,147,156,157], 1,1,1,2-Tetrafluoroethane [158], helium [159], carbon dioxide [159], oxygen [159], and combustion [141,148,160] flow fields. Since the advent of FLEET, its measurement potential has been fully explored. FLEET can be used not only for velocity measurement but also for measurements of other parameters in the flow field. For example,

by measuring the FLEET spectra, based on two-line thermometry, the flow field temperature can be obtained [150,157]. By analyzing the FLEET images, the boundary layer [146,161], shear layer [147,162], vorticity [163], and mixture fraction [156] can be obtained. By analyzing the FLEET signal intensity and lifetime, the pressure information of the flow field can be inverted [164].

The FLEET technique has the following advantages. Firstly, FLEET can achieve velocity measurement with only one fs laser, whose experimental system is simple. Secondly, FLEET uses fs laser as a light source, which can induce efficient multi-photon photolysis, therefore, it can be used to realize multi-dimensional measurement [140,153,165]. Thirdly, FLEET uses molecular nitrogen as a tracer, so the interference on the reactions of the flow field can be minimized. Fourthly, FLEET enables the measurement of other parameters in the flow field. However, there are still some technical defects in the current FLEET technique, such as poor signal-to-noise ratio (SNR). Many researchers have tried to enhance the signal intensity by using different wavelengths or adding inert gases [139]. At present, the most effective way to enhance signal intensity is using laser-induced chemiluminescence of the radicals that have strong emission intensity.

Another fs-laser-based tagging velocimetry is femtosecond laser-induced cyano chemiluminescence (FLICC) [166], which is proposed by our group. When an fs laser focused at methane-seeded nitrogen gas flows, the high-intensity emission originating from CN ($B^2\Sigma^+ \rightarrow X^2\Sigma^+$) fluorescence was observed. The emission is strong and can last for hundreds of microseconds with a proper methane concentration. Therefore, velocity measurement can be achieved through CN fluorescence imaging. As shown in Figure 9, FLICC is an ideal tool for near-wall velocity measurements, which can be used to study, e.g., the boundary layer structure in supersonic flows. Although the FLICC technique requires hydrocarbons to be seeded in the measured flow field, it has a natural advantage when it comes to combustion flow fields.

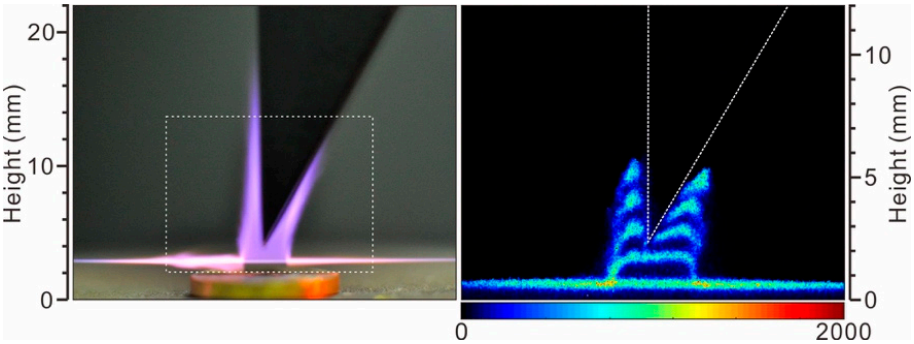


**Figure 9.** Following the movement of femtosecond laser-induced cyano chemiluminescence (FLICC) signal using a single lens reflex camera (**left**) and an ICCD camera in the on-chip multi-exposure mode (**right**).

## 5. Femtosecond Lasers Guided High Voltage Electric Discharges

In addition to the above-mentioned fs-laser-based techniques, fs lasers can also be used to guide high voltage electric discharges, which can be used for flow field measurements and plasma applications. Plasma is widely used in the fields of industry [167], environment [168], and medical science [169,170] due to its conductive and germicidal properties. High voltage discharges are the most commonly used methods to generate plasma, such as corona discharge [171,172], spark discharge [173], and dielectric barrier discharge [174,175]. Under atmospheric or high pressures, electric discharge in the air can form a long thin filamentary volume of ionized plasma [176]. However, no matter the kind of discharges, they are all based on a strong electrical field, which suffers the problem of random discharges in both time and space. Controlling the time and space of discharges simultaneously and accurately is so hard that it brings many limitations to its practical applications.

In the 1970s–1990s, researches on controlling high voltage discharges using pulse lasers have been reported [177]. The high voltage discharge can be well controlled in the air through nanosecond

laser guiding [178]. Due to the limitation of the Rayleigh range of the focused laser beam, discharge guidance over the range of about 1 m was achieved. The fs laser-induced filament appears to be ideally suitable for guiding a long-range atmospheric discharge.

Femtosecond laser-induced filament is the result of a dynamical competition between the Kerr effect and plasma defocus effect. The length of the filament depends on the femtosecond laser pulse energy and can be extended to several kilometers [13] when the laser energy is high enough. The long-distance transmission of the filament offers many potential applications. Wolf et al. [179] reported a free space laser telecommunication through the fog. They use a filament-induced shock wave to radially expel the droplets out of the beam from the air it sweeps, then providing a clean channel for telecom laser transmission, which has the potential to be applied to Earth-satellite free-space optical communications and secure ground-based optical communications.

The fs laser-induced filament is a weakly ionized plasma channel with a diameter of ~100 μm and an electron density of ~$10^{16}$ $cm^{-3}$ [180]. This plasma channel is weakly conductive and can be used for guiding high voltage discharges. The most practical application of fs laser-induced filament is laser-triggered switching. Many applications rely on the initiation of a well-controlled discharge between two charged electrodes, especially for high current equipment, where a gas-filled trigger is necessary. Since the first laser-triggered switching experiment in the early 1960s, a wide variety of spark gap geometries and laser types have been investigated. Using ns lasers to trigger discharges can achieve an excellent temporal stability of switched pulse with a jitter time of one nanosecond [181]. Better temporal stability, within picoseconds, was achieved by using an fs laser to trigger discharges [182,183], and the discharge path is strictly defined along the filament. Femtosecond laser-induced filament guiding discharge provides a safe, remote, and highly accurate controllable switch for high current equipment [184], which perfectly solves the problem of random discharges in both time and space.

Since the time and space of discharges can be accurately controlled, many applications based on laser-induced filament were developed [185,186]. Polynkin et al. [187] reported a multi-pulse scheme for laser-guided electrical breakdown of air, which is shown to be suitable for guiding discharges propagating in either direction or along curved paths. An example of curved discharges guided by timed sequences of three laser filaments in the dome and zigzag formations is shown in Figure 10, and a scheme for the guidance of natural lightning based on the application of multiple chirped femtosecond laser pulses was proposed.

Our group developed an fs laser-induced filament guiding discharges tagging velocimetry [188], named filamentary anemometry using femtosecond laser-extended electric discharge (FALED). FALED technique uses the filament to ignite a pulsed electric discharge between two electrodes. The laser-guided thin filamentary discharge plasma column was blown up perpendicularly by an air jet placed beneath in-between the two electrodes. The conductivity of the plasma channel was observed to sustain much longer so that a sequence of discharge filaments was generated as the plasma channel was blown up by the jet flow. The sequential bright thin discharge filaments can be photographed using a household camera to calculate the flow velocity distribution of the jet flow, as shown in Figure 11. The velocity measured by FALED agrees well with that measured by FLEET [188], and FALED has a better signal to noise ratio and a thinner tagged line. Compared with FLEET and FLICC, FALED largely extends the application scenario and does not suffer from quenching. Furthermore, it should be emphasized that the discharge current is supposed to be extremely low in order to reduce intrusiveness.

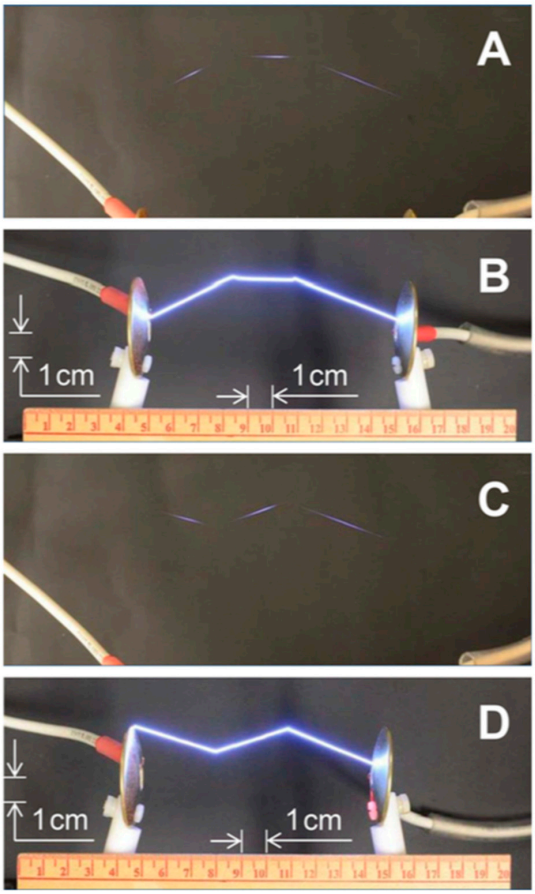


**Figure 10.** Examples of curved discharges guided by timed sequences of three laser filaments in the dome and zigzag formations. (**A**), (**C**) Photographs of fluorescence by the filament plasmas, averaged over 100 laser shots. (**B**), (**D**) Single-shot images of the corresponding guided discharges [187]. (Reproduced from Polynkin P, Multi-pulse scheme for laser-guided electrical breakdown of air. *Appl. Phys. Lett.* 2017, *111*, 161102, with the permission of AIP Publishing).

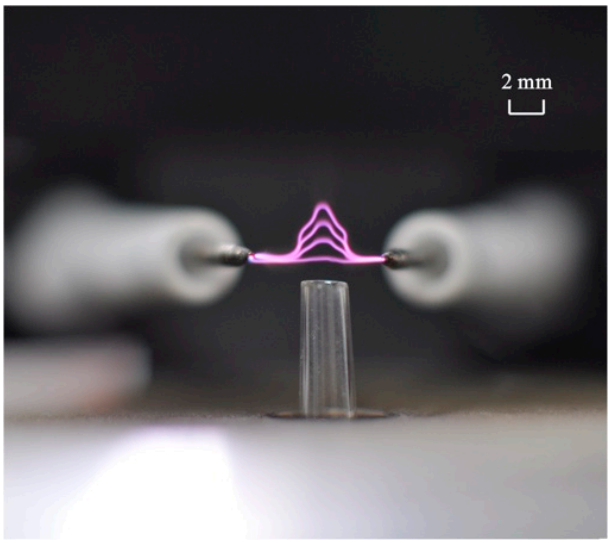


**Figure 11.** Filamentary anemometry using femtosecond laser-extended electric discharge (FALED) photo taken by the single lens reflex (SLR) camera of four sequential discharges with a separation of 40 μs and a gas flow speed of 35 m/s.

In summary, fs laser guiding discharges can have a lot of applications, such as laser-triggered switching, guiding natural lightning, and velocity measurements. There are many exciting phenomena that are worthy of examination. Shown in Figure 12 are spatially resolved plasma spectra of fs laser-induced filament guiding discharges. The plasma spectra indicate that the species in the discharged filament are totally different when the discharge current is changed by varying current limiting resistors. This phenomenon may be used to develop a method for species measurement with the potential to achieve one-dimensional measurement. The accurate controlling of discharges in both time and space also provides a possible way to study the spatiotemporal evolution processes of discharges plasma.

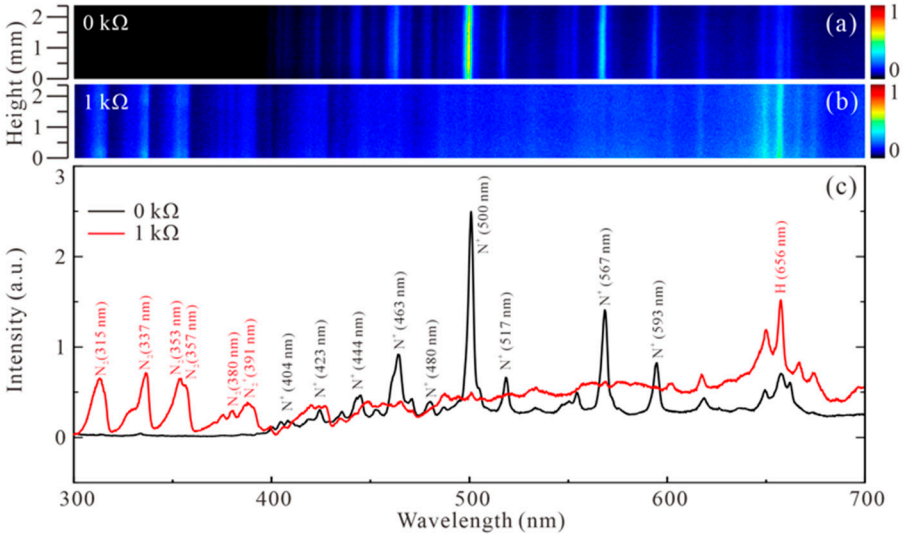


**Figure 12.** Emission spectra from the filamentary column of different plasmas collected with spectrometer slit, vertically orientated perpendicular to the thin plasma columns. (**a**) Imaging spectra of FALED with a resistance of 0 kΩ; (**b**) Imaging spectra of FALED along the jet flow with a resistance of 1 kΩ; (**c**) Spectral curve of emission from the filamentary plasma with the resistances of 0 kΩ (black line) and 1 kΩ (red line).

## 6. Conclusions

In summary, the development and application of a number of fs laser-based techniques for combustion and flow field diagnostics are reviewed. These novel techniques include fs two-photon laser-induced fluorescence (fs-TPLIF), fs laser-induced breakdown spectroscopy (fs-LIBS), fs laser electronic excitation tagging (FLEET), filament-induced nonlinear spectroscopy (FINS) and fs laser-induced plasma spectroscopy (FLIPS). In spite of their relatively short history, significant impacts of these techniques have been demonstrated in measuring velocity, temperature and intermediates in combustion and flow field.

However, there is still plenty of space for further development of these techniques, as all the techniques mentioned above have the temporal-resolved measurement capability, and the time resolution is in the range of nanosecond to sub-microsecond level. The fundamental mechanisms governing the chemical and physical processes introduced by the ultra-short laser pulse and ultra-high peak power are still to be investigated to form a knowledge-based understanding of the interaction between the fs laser and the combustion flow field and the mechanisms of filamentary electric discharge guided by fs lasers. It is predicted that the fs laser-based technologies will play an important role in combustion and flow field diagnostics in the near future.

**Author Contributions:** Conceptualization, Z.L.; Resources, D.Z., J.L. and Y.T.; Data curation, D.Z.; Writing-original draft preparation, B.L., D.Z. and Z.L.; Writing-review and editing, Z.L., B.L. and Q.G.; Supervision, Q.G. and Z.L.

**Funding:** This work was financially supported by the National Natural Science Foundation of China (NSFC) (91741205, 51776137).

**Conflicts of Interest:** The authors declare no conflict of interest.

## References


1. Mock, R.; Meixner, H. A miniaturized high-temperature pressure sensor for the combustion chamber of a spark ignition engine. *Sens. Actuators A* **1990**, *25*, 103–106. [CrossRef]
2. Klopfenstein, R., Jr. Air velocity and flow measurement using a Pitot tube. *ISA Trans.* **1998**, *37*, 257–263. [CrossRef]
3. Heitor, M.V.; Moreira, A.L.N. Thermocouples and sample probes for combustion studies. *Prog. Energy Combust. Sci.* **1993**, *19*, 259–278. [CrossRef]
4. Aldén, M.; Bood, J.; Li, Z.; Richter, M. Visualization and understanding of combustion processes using spatially and temporally resolved laser diagnostic techniques. *Proc. Combust. Inst.* **2011**, *33*, 69–97. [CrossRef]
5. Kohse-Höinghaus, K.; Barlow, R.S.; Aldén, M.; Wolfrum, J. Combustion at the focus: Laser diagnostics and control. *Proc. Combust. Inst.* **2005**, *30*, 89–123. [CrossRef]
6. Hanson, R.K.; Seitzman, J.M.; Paul, P.H. Planar laser-fluorescence imaging of combustion gases. *Appl. Phys. B* **1990**, *50*, 441–454. [CrossRef]
7. Crosley, D.R.; Smith, G.P. Laser-induced fluorescence spectroscopy for combustion diagnostics. *Opt. Eng.* **1983**, *22*, 545–553. [CrossRef]
8. Aldén, M.; Omrane, A.; Richter, M.; Särner, G. Thermographic phosphors for thermometry: A survey of combustion applications. *Prog. Energy Combust. Sci.* **2011**, *37*, 422–461. [CrossRef]
9. Chan, V.S.S.; Turner, J.T. Velocity measurement inside a motored internal combustion engine using three-component laser Doppler anemometry. *Opt. Laser Technol.* **2000**, *32*, 557–566. [CrossRef]
10. Shaddix, C.R.; Smyth, K.C. Laser-induced incandescence measurements of soot production in steady and flickering methane, propane, and ethylene diffusion flames. *Combust. Flame* **1996**, *107*, 418–452. [CrossRef]
11. Spence, D.E.; Kean, P.N.; Sibbett, W. 60-fsec pulse generation from a self-mode-locked Ti: Sapphire laser. *Opt. Lett.* **1991**, *16*, 42–44. [CrossRef] [PubMed]
12. Chin, S.L.; Xu, H. Tunnel ionization, population trapping, filamentation and applications. *J. Phys. B At. Mol. Opt. Phys.* **2016**, *49*, 222003. [CrossRef]
13. Chin, S.L. *Femtosecond Laser Filamentation*; Springer: New York, NY, USA, 2010; Volume 55, p. 137.
14. Eckbreth, A.C. Recent advances in laser diagnostics for temperature and species concentration in combustion. *Symp. Combust.* **1981**, *18*, 1471–1488. [CrossRef]
15. Hassel, E.P.; Linow, S. Laser diagnostics for studies of turbulent combustion. *Meas. Sci. Technol.* **2000**, *11*, R37. [CrossRef]
16. Hanson, R.K. Combustion diagnostics: Planar imaging techniques. *Symp. Combust.* **1986**, *21*, 1677–1691. [CrossRef]
17. Lucht, R.P.; Salmon, J.T.; King, G.B.; Sweeney, D.W.; Laurendeau, N.M. Two-photon-excited fluorescence measurement of hydrogen atoms in flames. *Opt. Lett.* **1983**, *8*, 365–367. [CrossRef] [PubMed]
18. Gathen, V.S.V.D.; Niemi, K. Absolute atomic oxygen density measurements by two-photon absorption laser-induced fluorescence spectroscopy in an RF-excited atmospheric pressure plasma jet. *Plasma Sources Sci. Technol.* **2005**, *14*, 375.
19. Rosell, J.; Sjöholm, J.; Richter, M.; Aldén, M. Comparison of three schemes of two-photon laser-induced fluorescence for CO detection in flames. *Appl. Spectrosc.* **2013**, *67*, 314–320. [CrossRef]
20. Bokor, J.; Freeman, R.R.; White, J.C.; Storz, R.H. Two-photon excitation of the level in H and D atoms. *Phys. Rev. A At. Mol. Opt. Phys.* **1981**, *24*, 612–614. [CrossRef]
21. Aldén, M.; Edner, H.; Grafström, P.; Svanberg, S. Two-photon excitation of atomic oxygen in a flame. *Opt. Commun.* **1982**, *42*, 244–246. [CrossRef]
22. Bischel, W.K.; Perry, B.E.; Crosley, D.R. Two-photon laser-induced fluorescence in oxygen and nitrogen atoms. *Chem. Phys. Lett.* **1981**, *82*, 85–88. [CrossRef]
23. DiMauro, L.F.; Gottscho, R.A.; Miller, T.A. Two-photon laser-induced fluorescence monitoring of O atoms in a plasma etching environment. *J. Appl. Phys.* **1984**, *56*, 2007–2011. [CrossRef]

24. Kulatilaka, W.D.; Frank, J.H.; Patterson, B.D.; Settersten, T.B. Analysis of 205-nm photolytic production of atomic hydrogen in methane flames. *Appl. Phys. B* **2009**, *97*, 227–242. [CrossRef]
25. Li, B.; Jonsson, M.; Algotsson, M.; Bood, J.; Li, Z.S.; Johansson, O.; Aldén, M.; Tunér, M.; Johansson, B. Quantitative detection of hydrogen peroxide in an HCCI engine using photofragmentation laser-induced fluorescence. *Proc. Combust. Inst.* **2013**, *34*, 3573–3581. [CrossRef]
26. Li, B.; Zhang, D.; Yao, M.; Li, Z. Strategy for single-shot $CH_3$ imaging in premixed methane/air flames using photofragmentation laser-induced fluorescence. *Proc. Combust. Inst.* **2017**, *36*, 4487–4495. [CrossRef]
27. Li, B.; Li, X.; Zhang, D.; Gao, Q.; Yao, M.; Li, Z. Comprehensive CO detection in flames using femtosecond two-photon laser-induced fluorescence. *Opt. Express* **2017**, *25*, 25809–25818. [CrossRef]
28. Settersten, T.B.; Dreizler, A.; Farrow, R.L. Temperature- and species-dependent quenching of CO B probed by two-photon laser-induced fluorescence using a picosecond laser. *J. Chem. Phys.* **2002**, *117*, 3173–3179. [CrossRef]
29. Frank, J.H.; Settersten, T.B. Two-photon LIF imaging of atomic oxygen in flames with picosecond excitation. *Proc. Combust. Inst.* **2005**, *30*, 1527–1534. [CrossRef]
30. Kulatilaka, W.D.; Gord, J.R.; Katta, V.R.; Roy, S. Photolytic-interference-free, femtosecond two-photon fluorescence imaging of atomic hydrogen. *Opt. Lett.* **2012**, *37*, 3051–3053. [CrossRef]
31. Stauffer, H.U.; Kulatilaka, W.D.; Gord, J.R.; Roy, S. Laser-induced fluorescence detection of hydroxyl (OH) radical by femtosecond excitation. *Opt. Lett.* **2011**, *36*, 1776–1778. [CrossRef]
32. Stauffer, H.U.; Gord, J.R.; Roy, S.; Kulatilaka, W.D. Detailed calculation of hydroxyl (OH) radical two-photon absorption via broadband ultrafast excitation. *J. Opt. Soc. Am. B Opt. Phys.* **2011**, *29*, 40–52. [CrossRef]
33. Wang, Y.; Jain, A.; Kulatilaka, W. CO imaging in piloted liquid-spray flames using femtosecond two-photon LIF. *Proc. Combust. Inst.* **2019**, *37*, 1305–1312. [CrossRef]
34. Wang, Y.; Kulatilaka, W.D. Detection of carbon monoxide (CO) in sooting hydrocarbon flames using femtosecond two-photon laser-induced fluorescence (fs-TPLIF). *Appl. Phys. B* **2018**, *124*. [CrossRef]
35. Rahman, K.A.; Patel, K.S.; Slipchenko, M.N.; Meyer, T.R.; Zhang, Z.; Wu, Y.; Gord, J.R.; Roy, S. Femtosecond, two-photon, laser-induced fluorescence (TP-LIF) measurement of CO in high-pressure flames. *Appl. Opt.* **2018**, *57*, 5666–5671. [CrossRef] [PubMed]
36. Wang, Y.; Kulatilak, W.D. Investigation of Femtosecond two-photon LIF of CO at elevated pressures. In *Laser Applications to Chemical, Security and Environmental Analysis*; Optical Society of America: Orlando, FL, USA, 2018.
37. Richardson, D.R.; Roy, S.; Gord, J.R. Femtosecond, two-photon, planar laser-induced fluorescence of carbon monoxide in flames. *Opt. Lett.* **2017**, *42*, 875–878. [CrossRef]
38. Richardson, D.R.; Roy, S.; Gord, J.R. Carbon monoxide femtosecond TALIF in turbulent flames. In Proceedings of the AIAA Aerospace Sciences Meeting, Kissimmee, FL, USA, 8–12 January 2018.
39. Jain, A.; Wang, Y.; Kulatilaka, W.D. Effect of H-atom concentration on soot formation in premixed ethylene/air flames. *Proc. Combust. Inst.* **2019**, *37*, 1289–1296. [CrossRef]
40. Jain, A.; Kulatilaka, W.D. Investigation of multi-photon excitation schemes for detecting atomic hydrogen in flames. In Proceedings of the 2018 Conference on Lasers and Electro-Optics (CLEO), San Jose, CA, USA, 13–18 May 2018; pp. 1–2.
41. Ding, P.; Ruchkina, M.; Liu, Y.; Alden, M.; Bood, J.; Department, O.P.; Lund, U.; Lunds, U.; Fysiska, I. Femtosecond two-photon-excited backward lasing of atomic hydrogen in a flame. *Opt. Lett.* **2018**, *43*, 1183–1186. [CrossRef]
42. Ding, P.; Ruchkina, M.; Liu, Y.; Ehn, A.; Alden, M.; Bood, J. Picosecond backward-propagating lasing of atomic hydrogen via femtosecond 2-photon-excitation in a flame. In Proceedings of the 2018 Conference on Lasers and Electro-Optics (CLEO), San Jose, CA, USA, 13–18 May 2018; pp. 1–2.
43. Ruchkina, M.; Ding, P.; Ehn, A.; Alden, M.; Bood, J. Spatially-resolved hydrogen atom detection in flames using backward lasing. In Proceedings of the 2018 Conference on Lasers and Electro-Optics (CLEO), San Jose, CA, USA, 13–18 May 2018; pp. 1–2.
44. Hall, C.A.; Kulatilaka, W.D.; Gord, J.R.; Pitz, R.W. Quantitative atomic hydrogen measurements in premixed hydrogen tubular flames. *Combust. Flame* **2014**, *161*, 2924–2932. [CrossRef]
45. Kulatilaka, W.D.; Gord, J.R.; Roy, S. Femtosecond two-photon LIF imaging of atomic species using a frequency-quadrupled Ti:sapphire laser. *Appl. Phys. B* **2014**, *116*, 7–13. [CrossRef]

46. Kulatilaka, W.; Roy, S.; Gord, J. Multi-photon fluorescence imaging of flame species using femtosecond excitation. In Proceedings of the Aerodynamic Measurement Technology, Ground Testing, and Flight Testing Conference, New Orleans, LA, USA, 25–28 June 2012.
47. Jain, A.; Kulatilaka, W.D. Two- and three-photon LIF detection of atomic hydrogen using femtosecond laser Pulses. In Proceedings of the Laser Applications to Chemical, Security and Environmental Analysis, Orlando, FL, USA, 25–28 June 2018.
48. Jain, A.; Wang, Y.; Kulatilaka, W.D. Spatially resolved atomic hydrogen concentration measurements in sooting hydrocarbon flames using femtosecond two-photon LIF. In Proceedings of the 33rd AIAA Aerodynamic Measurement Technology and Ground Testing Conference, Denver, CO, USA, 5–9 June 2017.
49. Schmidt, J.B.; Roy, S.; Kulatilaka, W.D.; Shkurenkov, I.; Adamovich, I.V.; Lempert, W.R.; Gord, J.R. Femtosecond, two-photon-absorption, laser-induced-fluorescence (fs-TALIF) imaging of atomic hydrogen and oxygen in non-equilibrium plasmas. *J. Phys. D Appl. Phys.* **2017**, *50*, 015204. [CrossRef]
50. Schmidt, J.B.; Kulatilaka, W.D.; Roy, S.; Frederickson, K.; Lempert, W.R.; Gord, J.R. Femtosecond TALIF imaging of atomic hydrogen in pulsed, non-equilibrium plasmas. In Proceedings of the 52nd Aerospace Sciences Meeting, National Harbor, MD, USA, 13–17 January 2015.
51. Li, B.; Zhang, D.; Li, X.; Gao, Q.; Yao, M.; Li, Z. Strategy of interference-free atomic hydrogen detection in flames using femtosecond multi-photon laser-induced fluorescence. *Int. J. Hydrog. Energy* **2017**, *42*, 3876–3880. [CrossRef]
52. Kulatilaka, W.D.; Roy, S.; Jiang, N.; Gord, J.R. Photolytic-interference-free, femtosecond, two-photon laser-induced fluorescence imaging of atomic oxygen in flames. *Appl. Phys. B* **2016**, *122*. [CrossRef]
53. Schmidt, J.B.; Sands, B.L.; Kulatilaka, W.D.; Roy, S.; Scofield, J.; Gord, J.R. Femtosecond, two-photon laser-induced-fluorescence imaging of atomic oxygen in an atmospheric-pressure plasma jet. *Plasma Sources Sci. Technol.* **2015**, *24*, 032004. [CrossRef]
54. Wang, Y.; Capps, C.; Kulatilaka, W.D. Mixture fraction imaging using femtosecond TPLIF of Krypton. In Proceedings of the AIAA Aerospace Sciences Meeting, Grapevine, TX, USA, 9–13 January 2017.
55. Wang, Y.; Kulatilaka, W.D. Two-photon laser induced fluorescence of krypton using femtosecond pulses. In Proceedings of the Conference on Lasers and Electro-Optics (CLEO), San Jose, CA, USA, 14–19 May 2017; pp. 1–2.
56. Wang, Y.; Capps, C.; Kulatilaka, W.D. Femtosecond two-photon laser-induced fluorescence of krypton for high-speed flow imaging. *Opt. Lett.* **2017**, *42*, 711–714. [CrossRef] [PubMed]
57. Richardson, D.R.; Jiang, N.; Stauffer, H.U.; Kearney, S.P.; Roy, S.; Gord, J.R. Mixture-fraction imaging at 1 kHz using femtosecond laser-induced fluorescence of krypton. *Opt. Lett.* **2017**, *42*, 3498–3501. [CrossRef] [PubMed]
58. Burluka, A. *Combustion Physics*; Wiley-VCH Verlag GmbH & Co. KGaA: Weinheim, Germany, 2010.
59. Settersten, T.B.; Dreizler, A.; Patterson, B.D.; Schrader, P.E.; Farrow, R.L. Photolytic interference affecting two-photon laser-induced fluorescence detection of atomic oxygen in hydrocarbon flames. *Appl. Phys. B* **2003**, *76*, 479–482. [CrossRef]
60. Singh, S.; Musculus, M.P.B.; Reitz, R.D. Mixing and flame structures inferred from OH-PLIF for conventional and low-temperature diesel engine combustion. *Combust. Flame* **2009**, *156*, 1898–1908. [CrossRef]
61. Donbar, J.M.; Driscoll, J.F.; Carter, C.D. Reaction zone structure in turbulent nonpremixed jet flames-from CH-OH PLIF images. *Combust. Flame* **2000**, *122*, 1–19. [CrossRef]
62. Li, Z.S.; Li, B.; Sun, Z.W.; Bai, X.S.; Aldén, M. Turbulence and combustion interaction: High resolution local flame front structure visualization using simultaneous single-shot PLIF imaging of CH, OH, and $CH_2O$ in a piloted premixed jet flame. *Combust. Flame* **2010**, *157*, 1087–1096. [CrossRef]
63. Duwig, C.; Li, B.; Li, Z.S.; Aldén, M. High resolution imaging of flameless and distributed turbulent combustion. *Combust. Flame* **2012**, *159*, 306–316. [CrossRef]
64. Laurendeau, N.M.; Goldsmith, J.E.M. Comparison of hydroxyl concentration profiles using five laser-induced fluorescence methods in a lean subatmospheric-pressure $H_2/O_2$/Ar flame. *Combust. Sci. Technol.* **1989**, *63*, 139–152. [CrossRef]
65. Renfro, M.W.; Guttenfelder, W.A.; King, G.B.; Laurendeau, N.M. Scalar time-series measurements in turbulent $CH_4/H_2/N_2$ nonpremixed flames: OH. *Combust. Flame* **2000**, *123*, 389–401. [CrossRef]
66. Westblom, U.; Bengtsson, P.E.; Aldén, M. Carbon atom fluorescence and $C_2$ emission detected in fuel-rich flames using a UV laser. *Appl. Phys. B* **1991**, *52*, 371–375. [CrossRef]

67. Das, P.; Ondrey, G.S.; van Veen, N.; Bersohn, R. Two photon laser induced fluorescence of carbon atoms. *J. Chem. Phys.* **1983**, *79*, 724–726. [CrossRef]
68. Zhang, D.Y.; Gao, Q.; Li, B.; Li, Z.S. Ammonia measurements with femtosecond laser-induced plasma spectroscopy. *Appl. Opt. B* **2019**, *58*, 1210–1214. [CrossRef]
69. Bol'Shakov, A.A.; Yoo, J.H.; Liu, C.; Plumer, J.R.; Russo, R.E. Laser-induced breakdown spectroscopy in industrial and security applications. *Appl. Opt.* **2010**, *49*, C132–C142. [CrossRef]
70. Choi, I.; Chan, G.C.Y.; Mao, X.; Perry, D.L.; Russo, R.E. Line selection and parameter optimization for trace analysis of uranium in glass matrices by laser-induced breakdown spectroscopy (LIBS). *Appl. Spectrosc.* **2013**, *67*, 1275–1284. [CrossRef]
71. Bonta, M.; Gonzalez, J.J.; Quarles, C.D., Jr.; Russo, R.E.; Hegedus, B.; Limbeck, A. Elemental mapping of biological samples by the combined use of LIBS and LA-ICP-MS. *J. Anal. At. Spectrom.* **2016**, *1*, 252–258. [CrossRef]
72. Rehse, S.J.; Salimnia, H.; Miziolek, A.W. Laser-induced breakdown spectroscopy (LIBS): An overview of recent progress and future potential for biomedical applications. *J. Med. Eng. Technol.* **2012**, *36*, 77–89. [CrossRef] [PubMed]
73. Singh, M.; Karki, V.; Mishra, R.K.; Kumar, A.; Kaushik, C.P.; Mao, X.; Russo, R.E.; Sarkar, A. Analytical spectral dependent partial least squares regression: A study of nuclear waste glass from thorium based fuel using LIBS. *J. Anal. At. Spectrom.* **2015**, *3*, 2507–2515. [CrossRef]
74. Quarles, C.D.; Gonzalez, J.J.; East, L.J.; Yoo, J.H.; Morey, M.; Russo, R.E. Fluorine analysis using Laser Induced Breakdown Spectroscopy (LIBS). *J. Anal. At. Spectrom.* **2014**, *29*, 1238–1242. [CrossRef]
75. Colao, F.; Fantoni, R.; Lazic, V.; Paolini, A.; Fabbri, F.; Ori, G.G.; Marinangeli, L.; Baliva, A. Investigation of LIBS feasibility for in situ planetary exploration: An analysis on Martian rock analogues. *Planet. Space Sci.* **2004**, *52*, 117–123. [CrossRef]
76. Harmon, R.S.; Remus, J.; McMillan, N.J.; McManus, C.; Collins, L.; Gottfried, L.J.L., Jr.; DeLucia, F.C.; Miziolek, A.W. LIBS analysis of geomaterials: Geochemical fingerprinting for the rapid analysis and discrimination of minerals. *Appl. Geochem.* **2009**, *24*, 1125–1141. [CrossRef]
77. Gaudiuso, R.; Dell'Aglio, M.; De Pascale, O.; Senesi, G.S.; De Giacomo, A. Laser induced breakdown spectroscopy for elemental analysis in environmental, cultural heritage and space applications: A review of methods and results. *Sensors* **2010**, *10*, 7434–7468. [CrossRef] [PubMed]
78. Haddad, J.E.; Canioni, L.; Bousquet, B. Good practices in LIBS analysis: Review and advices. *Spectrochim. Acta B* **2014**, *101*, 171–182. [CrossRef]
79. Michel, A.P.M. Review: Applications of single-shot laser-induced breakdown spectroscopy. *Spectrochim. Acta B* **2010**, *65*, 185–191. [CrossRef]
80. Rhodes, W.T. Laser-induced breakdown spectroscopy. In *Springer Series in Optical Sciences*; Springer: Berlin, Germany, 2014.
81. Cremers, D.A.; Multari, R.A.; Knight, A.K. Laser-induced breakdown spectroscopy. In *Encyclopedia of Analytical Chemistry*; 2016; Available online: https://onlinelibrary.wiley.com/doi/10.1002/9780470027318.a5110t.pub3/figures (accessed on 25 April 2019).
82. Tian, Z.; Dong, M.; Li, S.; Lu, J. Spatially resolved laser-induced breakdown spectroscopy in laminar premixed methane-air flames. *Spectrochim. Acta B* **2017**, *136*, 8–15. [CrossRef]
83. Kiefer, J.; Zhou, B.; Li, Z.; Aldén, M. Impact of plasma dynamics on equivalence ratio measurements by laser-induced breakdown spectroscopy. *Appl. Opt.* **2015**, *54*, 4221–4226. [CrossRef]
84. Michalakou, A.; Stavropoulos, P.; Couris, S. Laser-induced breakdown spectroscopy in reactive flows of hydrocarbon-air mixtures. *Appl. Phys. Lett.* **2008**, *92*, 081501. [CrossRef]
85. Do, H.; Carter, C.D.; Liu, Q.; Ombrello, T.M.; Hammack, S.; Lee, T.; Hsu, K.Y. Simultaneous gas density and fuel concentration measurements in a supersonic combustor using laser induced breakdown. *Proc. Combust. Inst.* **2015**, *35*, 2155–2162. [CrossRef]
86. Zimmer, L.; Yoshida, S. Feasibility of laser-induced plasma spectroscopy for measurements of equivalence ratio in high-pressure conditions. *Exp. Fluids* **2012**, *52*, 891–904. [CrossRef]
87. Ferioli, F.; Buckley, S.G. Measurements of hydrocarbons using laser-induced breakdown spectroscopy. *Combust. Flame* **2006**, *144*, 435–447. [CrossRef]
88. Kotzagianni, M.; Yuan, R.; Mastorakos, E.; Couris, S. Laser-induced breakdown spectroscopy measurements of mean mixture fraction in turbulent methane flames with a novel calibration scheme. *Combust. Flame* **2016**, *167*, 72–85. [CrossRef]

89. Labutin, T.A.; Lednev, V.N.; Ilyincd, A.A.; Popov, A.M. Femtosecond laser-induced breakdown spectroscopy. *J. Anal. At. Spectrom.* **2016**, *31*, 90–118. [CrossRef]
90. Kotzagianni, M.; Couris, S. Femtosecond laser induced breakdown spectroscopy of air-methane mixtures. *Chem. Phys. Lett.* **2013**, *561–562*, 36–41. [CrossRef]
91. Patnaik, A.K.; Wu, Y.; Hsu, P.S.; Gragston, M.; Zhang, Z.; Gord, J.R.; Roy, S. Simultaneous LIBS signal and plasma density measurement for quantitative insight into signal instability at elevated pressure. *Opt. Express* **2018**, *26*, 25750. [CrossRef] [PubMed]
92. Patnaik, A.K.; Hsu, P.S.; Stolt, A.J.; Estevadeordal, J.; Gord, J.R.; Roy, S. Advantages of ultrafast LIBS for high-pressure diagnostics. *Imaging Appl. Opt.* **2018**. [CrossRef]
93. Kotzagianni, M.; Couris, S. Femtosecond laser induced breakdown for combustion diagnostics. *Appl. Phys. Lett.* **2012**, *100*, 264104. [CrossRef]
94. Couris, S.; Kotzagianni, M.; Baskevicius, A.; Bartulevicius, T.; Sirutkaitis, V. Combustion diagnostics with femtosecond laser radiation. *J. Phys.* **2014**, *548*, 12056. [CrossRef]
95. Patnaik, A.K.; Hsu, P.S.; Roy, S.; Wu, Y.; Gragston, M.; Zhang, Z.; Gord, J.R. Ultrafast laser-induced-breakdown spectroscopy (LIBS) for F/A-ratio measurement of hydrocarbon flames. In Proceedings of the AIAA Aerospace Sciences Meeting, Kissimmee, FL, USA, 8–12 January 2018.
96. Braun, A.; Korn, G.; Liu, X.; Du, D.; Squier, J.; Mourou, G. Self-channeling of high-peak-power femtosecond laser pulses in air. *Opt. Lett.* **1995**, *20*, 73–75. [CrossRef]
97. Kasparian, J.; Wolf, J.P. Physics and applications of atmospheric nonlinear optics and filamentation. *Opt. Express* **2008**, *16*, 466–493. [CrossRef]
98. Couairon, A.; Mysyrowicz, A. Femtosecond filamentation in transparent media. *Phys. Rep.* **2007**, *441*, 47–189. [CrossRef]
99. Xu, H.L.; Daigle, J.F.; Luo, Q.; Chin, S.L. Femtosecond laser-induced nonlinear spectroscopy for remote sensing of methane. *Appl. Phys. B* **2006**, *82*, 655–658. [CrossRef]
100. Xu, H.; Cheng, Y.; Chin, S.; Sun, H. Femtosecond laser ionization and fragmentation of molecules for environmental sensing. *Laser Photonics Rev.* **2015**, *9*, 275–293. [CrossRef]
101. Li, H.; Jiang, Y.; Li, S.; Chen, A.; Li, S.; Jin, M. Research on the fluorescence emission from water vapor induced by femtosecond filamentation in air. *Chem. Phys. Lett.* **2016**, *662*, 188–191. [CrossRef]
102. Li, H.; Zang, H.; Xu, H.; Sun, H.; Baltuška, A.; Polynkin, P. Robust Remote sensing of trace-level heavy-metal contaminants in water using laser filaments. *Glob. Chall.* **2018**, *3*, 1800070. [CrossRef]
103. Li, H.L.; Xu, H.L.; Yang, B.S.; Chen, Q.D.; Zhang, T.; Sun, H.B. Sensing combustion intermediates by femtosecond filament excitation. *Opt. Lett.* **2013**, *38*, 1250–1252. [CrossRef] [PubMed]
104. Li, H.; Wei, X.; Xu, H.; Chin, S.; Yamanouchi, K.; Sun, H. Femtosecond laser filamentation for sensing combustion intermediates: A comparative study. *Sens. Actuators B Chem.* **2014**, *203*, 887–890. [CrossRef]
105. Li, H.; Chu, W.; Xu, H.; Cheng, Y.; Chin, S.; Yamanouchi, K.; Sun, H. Simultaneous identification of multi-combustion-intermediates of alkanol-air flames by femtosecond filament excitation for combustion sensing. *Sci. Rep.* **2016**, *6*, 27340. [CrossRef]
106. Li, S.; Li, Y.; Shi, Z.; Sui, L.; Li, H.; Li, Q.; Chen, A.; Jiang, Y.; Jin, M. Fluorescence emission induced by the femtosecond filament transmitting through the butane/air flame. *Spectrochim. Acta A* **2018**, *189*, 32–36. [CrossRef] [PubMed]
107. Li, H.; Chu, W.; Zang, H.; Xu, H.; Cheng, Y.; Chin, S.L. Critical power and clamping intensity inside a filament in a flame. *Opt. Express* **2016**, *24*, 3424. [CrossRef] [PubMed]
108. Chu, W.; Li, H.; Ni, J.; Zeng, B.; Yao, J.; Zhang, H.; Li, G.; Jing, C.; Xie, H.; Xu, H.; et al. Lasing action induced by femtosecond laser filamentation in ethanol flame for combustion diagnosis. *Appl. Phys. Lett.* **2014**, *104*, 91106. [CrossRef]
109. Zang, H.; Li, H.; Su, Y.; Fu, Y.; Hou, M.; Baltuška, A.; Yamanouchi, K.; Xu, H. Third-harmonic generation and scattering in combustion flames using a femtosecond laser filament. *Opt. Lett.* **2018**, *43*, 615–618. [CrossRef] [PubMed]
110. Hartung, G.; Hult, J.; Kaminski, C.F. A flat flame burner for the calibration of laser thermometry techniques. *Meas. Sci. Technol.* **2006**, *17*, 2485–2493. [CrossRef]
111. Liu, X.; Lu, X.; Liu, X.; Xi, T.; Liu, F.; Ma, J.; Zhang, J. Tightly focused femtosecond laser pulse in air: From filamentation to breakdown. *Opt. Express* **2010**, *18*, 26007–26017. [CrossRef] [PubMed]

112. Hsu, P.S.; Patnaik, A.K.; Stolt, A.J.; Estevadeordal, J.; Roy, S.; Gord, J.R. Femtosecond-laser-induced plasma spectroscopy for high-pressure gas sensing: Enhanced stability of spectroscopic signal. *Appl. Phys. Lett.* **2018**, *113*, 214103. [CrossRef]
113. Zhang, D.; Gao, Q.; Li, B.; Zhu, Z.; Li, Z. Instantaneous one-dimensional equivalence ratio measurements in methane/air mixtures using femtosecond laser-induced plasma spectroscopy. *Opt. Express* **2019**, *27*, 2159–2169. [CrossRef] [PubMed]
114. Bruun, H.H. Hot-wire anemometry: Principles and Signal Analysis. *Meas. Sci. Technol.* **1996**, 7. [CrossRef]
115. Westerweel, J.; Elsinga, G.E.; Adrian, R.J. Particle image velocimetry for complex and turbulent flows. *Annu. Rev. Fluid Mech.* **2013**, *45*, 409–436. [CrossRef]
116. Wereley, S.T.; Meinhart, C.D. Recent advances in micro-particle image velocimetry. *Annu. Rev. Fluid Mech.* **2010**, *42*, 557–576. [CrossRef]
117. Tropea, C. Laser Doppler anemometry: Recent developments and future challenges. *Meas. Sci. Technol* **1995**, *6*, 605–619. [CrossRef]
118. Chen, F.; Li, H.; Hu, H. Molecular tagging techniques and their applications to the study of complex thermal flow phenomenal, 211. *Acta. Mech. Sin.* **2015**, *31*, 425–445. [CrossRef]
119. Lempert, W.R.; Jiang, N.; Sethuram, S.; Mo, S. Molecular tagging velocimetry measurements in supersonic microjets. *AIAA J.* **2015**, *40*, 1065–1070. [CrossRef]
120. Mittal, M.; Sadr, R.; Schock, H.J.; Fedewa, A.; Naqwi, A. In-cylinder engine flow measurement using stereoscopic molecular tagging velocimetry (SMTV). *Exp. Fluids* **2009**, *46*, 277–284. [CrossRef]
121. Krüger, S.; Grünefeld, G. Stereoscopic flow-tagging velocimetry. *Appl. Phys. B* **1999**, *69*, 509–512. [CrossRef]
122. Pan, F.; Sanchez-Gonzalez, R.; McIlvoy, M.H.; Bowersox, R.D.; North, S.W. Simultaneous three-dimensional velocimetry and thermometry in gaseous flows using the stereoscopic vibrationally excited nitric oxide monitoring technique. *Opt. Lett.* **2016**, *41*, 1376–1379. [CrossRef] [PubMed]
123. Sanchez-Gonzalez, R.; Bowersox, R.D.; North, S.W. Simultaneous velocity and temperature measurements in gaseous flowfields using the vibrationally excited nitric oxide monitoring technique: A comprehensive study. *Appl. Opt.* **2012**, *51*, 1216–1228. [CrossRef]
124. Rubinsztein-Dunlop, H.; Littleton, B.; Barker, P.; Ljungberg, P.; Malmsten, Y. Ionic strontium fluorescence as a method for flow tagging velocimetry. *Exp. Fluids* **2001**, *30*, 36–42. [CrossRef]
125. Barker, P.; Thomas, A.; Rubinsztein-Dunlop, H.; Ljungberg, P. Velocity measurements by flow tagging employing laser enhanced ionisation and laser induced fluorescence. *Spectrochim. Acta B* **1995**, *50*, 1301–1310. [CrossRef]
126. Miles, R.B.; Grinstead, J.; Kohl, R.H.; Diskin, G. The RELIEF flow tagging technique and its application in engine testing facilities and for helium-air mixing studies. *Meas. Sci. Technol.* **2000**, *11*, 1272–1281. [CrossRef]
127. Miles, R.; Cohen, C.; Connors, J.; Howard, P.; Huang, S. Velocity measurements by vibrational tagging and fluorescent probing of oxygen. *Opt. Lett.* **1987**, *11*, 861–863. [CrossRef]
128. Dam, N.; Kleindouwel, R.J.; Sijtsema, N.M.; Meulen, J.J. Nitric oxide flow tagging in unseeded air. *Opt. Lett.* **2001**, *26*, 36–38. [CrossRef] [PubMed]
129. Pitz, R.W.; Ribarov, L.A.; Wehrmeyer, J.A.; Batliwala, F.; Debarber, P.A. Ozone tagging velocimetry using narrowband excimer lasers. *AIAA J.* **1999**, *37*, 708–714.
130. Pitz, R.W.; Brown, T.M.; Nandula, S.P.; Skaggs, P.A.; Debarber, P.A.; Brown, M.S.; Segall, J. Unseeded velocity measurement by ozone tagging velocimetry. *Opt. Lett.* **1996**, *21*, 755–757. [CrossRef] [PubMed]
131. Lahr, M.D.; Pitz, R.W.; Douglas, Z.W.; Carter, C.D. Hydroxyl-tagging-velocimetry measurements of a supersonic flow over a cavity. *J. Propuls. Power* **2010**, *26*, 790–797. [CrossRef]
132. Ribarov, L.A.; Wehrmeyer, J.A.; Pitz, R.W.; Yetter, R.A. Hydroxyl tagging velocimetry (HTV) in experimental air flows. *Appl. Phys. B* **2002**, *74*, 175–183. [CrossRef]
133. Boedeker, L.R. Velocity measurement by $H_2O$ photolysis and laser-induced fluorescence of OH. *Opt. Lett.* **1989**, *14*, 473–475. [CrossRef] [PubMed]
134. Michael, J.B.; Edwards, M.R.; Dogariu, A.; Miles, R.B. Femtosecond laser electronic excitation tagging for quantitative velocity imaging in air. *Appl. Opt.* **2011**, *26*, 5158–5162. [CrossRef]
135. Jiang, N.; Halls, B.R.; Stauffer, H.U.; Danehy, P.M.; Gord, J.R.; Roy, S. Selective two-photon absorptive resonance femtosecond-laser electronic-excitation tagging velocimetry. *Opt. Lett.* **2016**, *41*, 2225–2228. [CrossRef]

136. Reese, D.; Danehy, P. Application of STARFLEET velocimetry in the NASA langley 0.3-meter transonic cryogenic tunnel. In Proceedings of the Aerodynamic Measurement Technology and Ground Testing Conference, Atlanta, GA, USA, 25–29 June 2018.
137. Jiang, N.; Halls, B.R.; Stauffer, H.U.; Danehy, P.M.; Gord, J.R.; Roy, S. Selective two-photon absorptive resonance femtosecond-laser electronic-excitation tagging (STARFLEET) velocimetry in flow and combustion diagnostics. In Proceedings of the 32nd AIAA Aerodynamic Measurement Technology and Ground Testing Conference, Washington, DC, USA, 13–17 June 2016.
138. Jiang, N.; Stauffer, H.U.; Roy, S.; Danehy, P.M.; Halls, B.R.; Gord, J.R. Nitrogen molecular-tagging velocimetry techniques using ultrashort-pulse lasers. In Proceedings of the Laser Applications to Chemical, Security and Environmental Analysis, Heidelberg, Germany, 25–28 July 2016.
139. Zhang, Y.; Miles, R.B. Femtosecond laser tagging for velocimetry in argon and nitrogen gas mixtures. *Opt. Lett.* **2018**, *43*, 551–554. [CrossRef]
140. Pouya, S.; Van Rhijn, A.; Dantus, M.; Koochesfahani, M. Multi-photon molecular tagging velocimetry with femtosecond excitation (FemtoMTV). *Exp. Fluids* **2014**, *55*, 1791. [CrossRef]
141. Miles, R.B.; Edwards, M.R.; Michael, J.B.; Calvert, N.D.; Dogariu, A. Femtosecond laser electronic excitation tagging (FLEET) for imaging flow structure in unseeded hot or cold air or nitrogen. In Proceedings of the 51st AIAA Aerospace Sciences Meeting including the New Horizons Forum and Aerospace Exposition, Grapevine, TX, USA, 7–10 January 2013.
142. Burns, R.A.; Danehy, P.M. FLEET velocimetry measurements on a transonic airfoil. In Proceedings of the 55th AIAA Aerospace Sciences Meeting, Grapevine, TX, USA, 9–13 January 2017.
143. Burns, R.A.; Danehy, P.M.; Halls, B.R.; Jiang, N. Femtosecond laser electronic excitation tagging velocimetry in a transonic, cryogenic wind tunnel. *AIAA J.* **2016**, *55*, 680–685. [CrossRef]
144. Burns, R.; Danehy, P.M.; Jones, S.B.; Halls, B.R.; Jiang, N. Application of FLEET velocimetry in the NASA langley 0.3-meter transonic cryogenic tunnel. In Proceedings of the 31st AIAA Aerodynamic Measurement Technology and Ground Testing Conference, Dallas, TX, USA, 22–26 June 2015.
145. Dogariu, L.; Dogariu, A.; Smith, M.S.; Marineau, E.C.; Miles, R.B. Hypersonic flow velocity measurements using FLEET. In Proceedings of the 2018 Conference on Lasers and Electro-Optics (CLEO), San Jose, CA, USA, 13–18 May 2018.
146. Dogariu, L.E.; Dogariu, A.; Miles, R.B.; Smith, M.S.; Marineau, E.C. Non-intrusive hypersonic freestream and turbulent boundary-layer velocity measurements in AEDC tunnel 9 using FLEET. In Proceedings of the AIAA Aerospace Sciences Meeting, Kissimmee, FL, USA, 8–12 January 2018.
147. Zhang, Y.; Miles, R.B. Shear layer measurements along curved surfaces using the FLEET method. In Proceedings of the AIAA Aerospace Sciences Meeting, Kissimmee, FL, USA, 8–12 January 2018.
148. Deluca, N.J.; Miles, R.B.; Jiang, N.; Kulatilaka, W.D.; Patnaik, A.K.; Gord, J.R. FLEET velocimetry for combustion and flow diagnostics. *Appl. Opt.* **2017**, *56*, 8632–8638. [CrossRef]
149. Hsu, P.S.; Jiang, N.; Danehy, P.M.; Gord, J.R.; Roy, S. Fiber-coupled ultrashort-pulse-laser-based electronic-excitation tagging velocimetry. *Appl. Opt.* **2018**, *57*, 560–566. [CrossRef]
150. Edwards, M.R.; Dogariu, A.; Miles, R.B. Simultaneous temperature and velocity measurements in air with femtosecond laser tagging. *AIAA J.* **2015**, *53*, 2280–2288. [CrossRef]
151. Edwards, M.R.; Limbach, C.; Miles, R.B.; Tropina, A. Limitations on high-spatial resolution measurements of turbulence using femtosecond laser tagging. In Proceedings of the 53rd AIAA Aerospace Sciences Meeting, Kissimmee, FL, USA, 5–9 January 2015.
152. Burns, R.A.; Peters, C.J.; Danehy, P.M. Unseeded velocimetry in nitrogen for high-pressure, cryogenic wind tunnels: Part I. Femtosecond-laser tagging. *Meas. Sci. Technol.* **2018**, *29*, 115302. [CrossRef]
153. Zhang, Y.; Shneider, M.N.; Miles, R.B. Femtosecond laser excitation in argon-nitrogen mixtures. *AIAA J.* **2018**, *56*, 1060–1071. [CrossRef]
154. Zhang, Y.; Shneider, M.N.; Miles, R.B. Characterization of intermediate reactions following femtosecond laser excitation in argon-nitrogen mixtures. In Proceedings of the 55th AIAA Aerospace Sciences Meeting, Grapevine, TX, USA, 9–13 January 2017.
155. Zhang, Y.; Calvert, N.; Shneider, M.N.; Miles, R.B. Enhancement of FLEET in argon gas mixtures. In Proceedings of the 32nd AIAA Aerodynamic Measurement Technology and Ground Testing Conference, Washington, DC, USA, 13–17 June 2016.

156. Halls, B.R.; Jiang, N.; Gord, J.R.; Danehy, P.M.; Roy, S. Mixture-fraction measurements with femtosecond-laser electronic-excitation tagging. *Appl. Opt.* **2017**, *56*, E94–E98. [CrossRef] [PubMed]
157. Edwards, M.; Dogariu, A.; Miles, R. Simultaneous temperature and velocity measurement in unseeded air flows with FLEET. In Proceedings of the 51st AIAA Aerospace Sciences Meeting including the New Horizons Forum and Aerospace Exposition, Grapevine, TX, USA, 7–10 January 2013.
158. Zhang, Y.; Miles, R.B.; Danehy, P.M. Femtosecond laser tagging in 1,1,1,2-Tetrafluoroethane with trace quantities of air. In Proceedings of the AIAA Aerospace Sciences Meeting, Kissimmee, FL, USA, 8–12 January 2018.
159. Calvert, N.; Zhang, Y.; Miles, R.B. Characterizing FLEET for aerodynamic measurements in various gas mixtures and non-air environments. In Proceedings of the 32nd AIAA Aerodynamic Measurement Technology and Ground Testing Conference, Washington, DC, USA, 13–17 June 2016.
160. Zhang, D.; Li, B.; Gao, Q.; Li, Z. Applicability of femtosecond laser electronic excitation tagging in combustion flow field velocity measurements. *Appl. Spectrosc.* **2018**, *72*, 1807–1813. [CrossRef]
161. Calvert, N.; Dogariu, A.; Miles, R.B. FLEET boundary layer velocity profile measurements. In Proceedings of the 44th AIAA Plasmadynamics and Lasers Conference, San Diego, CA, USA, 24–27 June 2013.
162. Zhang, Y.; Calvert, N.; Dogariu, A.; Miles, R.B. Towards shear flow measurements using FLEET. In Proceedings of the 54th AIAA Aerospace Sciences Meeting, San Diego, CA, USA, 4–8 January 2016.
163. Calvert, N.D.; Dogariu, A.; Miles, R.B. 2-D velocity and vorticity measurements with FLEET. In Proceedings of the 30th AIAA Aerodynamic Measurement Technology and Ground Testing Conference, Atlanta, GA, USA, 16–20 June 2014.
164. Burns, R.A.; Peters, C.J.; Danehy, P.M. Multiparameter flowfield measurements in high-pressure, cryogenic environments using femtosecond lasers. In Proceedings of the 32nd AIAA Aerodynamic Measurement Technology and Ground Testing Conference, Washington, DC, USA, 13–17 June 2016.
165. Danehy, P.M.; Bathel, B.F.; Calvert, N.D.; Dogariu, A.; Miles, R.B. Three component velocity and acceleration measurement using FLEET. In Proceedings of the 30th AIAA Aerodynamic Measurement Technology and Ground Testing Conference, Atlanta, GA, USA, 16–20 June 2014.
166. Li, B.; Zhang, D.; Li, X.; Gao, Q.; Zhu, Z.; Li, Z. Femtosecond laser-induced cyano chemiluminescence in methane-seeded nitrogen gas flows for near-wall velocimetry. *J. Phys. D Appl. Phys.* **2018**, *51*, 295102. [CrossRef]
167. Li, X.; Shi, C.; Xu, Y.; Zhang, X.; Wang, K.; Zhu, A. Pulsed streamer discharge plasma over Ni/HZSM-5 catalysts for methane conversion to aromatics at atmospheric pressure. *Plasma Process. Polym.* **2007**, *4*, 15–18. [CrossRef]
168. Naseh, M.V.; Khodadadi, A.A.; Mortazavi, Y.; Pourfayaz, F.; Alizadeh, O.; Maghrebi, M. Fast and clean functionalization of carbon nanotubes by dielectric barrier discharge plasma in air compared to acid treatment. *Carbon* **2010**, *48*, 1369–1379. [CrossRef]
169. Mandolfino, C.; Lertora, E.; Gambaro, C. Influence of cold plasma treatment parameters on the mechanical properties of polyamide homogeneous bonded joints. *Surf. Coat. Technol.* **2017**, *313*, 222–229. [CrossRef]
170. Machala, Z.; Janda, M.; Hensel, K.; Jedlovský, I.; Leštinská, L.; Foltin, V.; Martišovitš, V.; Morvová, M. Emission spectroscopy of atmospheric pressure plasmas for bio-medical and environmental applications. *J. Mol. Spectrosc.* **2007**, *243*, 194–201. [CrossRef]
171. Wang, T.; Wei, Y.; Liu, Y.; Chen, N.; Liu, Y.; Ju, J.; Sun, H.; Wang, C.; Lu, H.; Liu, J.; et al. Direct observation of laser guided corona discharges. *Sci. Rep.* **2016**, *5*, 18681. [CrossRef]
172. Roth, G.J.; Gundersen, M.A. Laser-induced fluorescence images of NO distribution after needle pulsed negative corona discharge. *IEEE Trans. Plasma Sci.* **2002**, *27*, 28–29. [CrossRef]
173. Ballal, D.R.; Lefebvre, A.H. The influence of spark discharge characteristics on minimum ignition energy in flowing gases. *Combust. Flame* **1975**, *24*, 99–108. [CrossRef]
174. Horvatic, V.; Michels, A.; Ahlmann, N.; Jestel, G.; Veza, D.; Vadla, C.; Franzke, J. Time- and spatially resolved emission spectroscopy of the dielectric barrier discharge for soft ionization sustained by a quasi-sinusoidal high voltage. *Anal. Bioanal. Chem.* **2015**, *407*, 6689–6696. [CrossRef]
175. Ambrico, P.F.; Ambrico, M.; Šimek, M.; Colaianni, A.; Dilecce, G.; De Benedictis, S. Laser triggered single streamer in a pin-to-pin coplanar dielectric barrier discharge. *Appl. Phys. Lett.* **2009**, *94*, 231501. [CrossRef]
176. Zhu, J.; Gao, J.; Li, Z.; Ehn, A.; Aldén, A.; Larsson, A.; Kusano, Y. Sustained diffusive alternating current gliding arc discharge in atmospheric pressure air. *Appl. Phys. Lett.* **2014**, *105*, 234102. [CrossRef]

177. Woodworth, J.R.; Frost, C.A.; Green, T.A. UV laser triggering of high-voltage gas switches. *J. Appl. Phys.* **1982**, *53*, 4734–4739. [CrossRef]
178. Zhang, C.; Shao, T.; Yan, P.; Zhou, Y. Nanosecond-pulse gliding discharges between point-to-point electrodes in open air. *Plasma Sources Sci. Technol.* **2014**, *23*, 35004. [CrossRef]
179. Schimmel, G.; Produit, T.; Mongin, D.; Kasparian, J.; Wolf, J. Free space laser telecommunication through fog. *Optica* **2018**, *5*, 1338. [CrossRef]
180. Théberge, F.; Liu, W.; Simard, P.T.; Becker, A.; Chin, S.L. Plasma density inside a femtosecond laser filament in air: Strong dependence on external focusing. *Phys. Rev. E* **2006**, *74*, 36406. [CrossRef]
181. Lechien, K.R.; Savage, M.E.; Anaya, V.; Bliss, D.E.; Clark, W.T.; Corley, J.P.; Feltz, G.; Garrity, J.E.; Guthrie, D.W.; Hodge, K.C. Development of a 5.4 MV laser triggered gas switch for multimodule, multimegampere pulsed power drivers. *Rev. Mod. Phys.* **2008**, *11*, 060402. [CrossRef]
182. Arantchouk, L.; Houard, A.; Brelet, Y.; Carbonnel, J.; Larour, J.; André, Y.B.; Mysyrowicz, A. A simple high-voltage high current spark gap with subnanosecond jitter triggered by femtosecond laser filamentation. *Appl. Phys. Lett.* **2013**, *102*, 163502. [CrossRef]
183. Luther, B.M.; Furfaro, L.; Klix, A.; Rocca, J.J. Femtosecond laser triggering of a sub-100 picosecond jitter high-voltage spark gap. *Appl. Phys. Lett.* **2001**, *79*, 3248–3250. [CrossRef]
184. Arantchouk, L.; Point, G.; Brelet, Y.; Larour, J.; Carbonnel, J.; André, Y.B.; Mysyrowicz, A.; Houard, A. Compact 180-kV Marx generator triggered in atmospheric air by femtosecond laser filaments. *Appl. Phys. Lett.* **2014**, *104*, 103506. [CrossRef]
185. Point, G.; Arantchouk, L.; Thouin, E.; Carbonnel, J.; Mysyrowicz, A.; Houard, A. Long-lived laser-induced arc discharges for energy channeling applications. *Sci. Rep.* **2017**, *7*, 13801. [CrossRef] [PubMed]
186. Clerici, M.; Hu, Y.; Lassonde, P.; Milián, C.; Couairon, A.; Christodoulides, D.N.; Chen, Z.; Razzari, L.; Vidal, F.; Légaré, F.; et al. Laser-assisted guiding of electric discharges around objects. *Sci. Adv.* **2015**, *1*, e1400111. [CrossRef] [PubMed]
187. Polynkin, P. Multi-pulse scheme for laser-guided electrical breakdown of air. *Appl. Phys. Lett.* **2017**, *111*, 161102. [CrossRef]
188. Li, B.; Tian, Y.; Gao, Q.; Zhang, D.; Li, X.; Zhu, Z.; Li, Z. Filamentary anemometry using femtosecond laser-extended electric discharge—FALED. *Opt. Express* **2018**, *26*, 21132. [CrossRef] [PubMed]